

2013-01-01

An Approach To Power Efficiency Determination In The Solar Energy Systems Using Central Composite Design And Box-Behnken Design

Juan Venegas Mendez

University of Texas at El Paso, jvenegasmendez@miners.utep.edu

Follow this and additional works at: https://digitalcommons.utep.edu/open_etd



Part of the [Industrial Engineering Commons](#), and the [Oil, Gas, and Energy Commons](#)

Recommended Citation

Venegas Mendez, Juan, "An Approach To Power Efficiency Determination In The Solar Energy Systems Using Central Composite Design And Box-Behnken Design" (2013). *Open Access Theses & Dissertations*. 1952.
https://digitalcommons.utep.edu/open_etd/1952

This is brought to you for free and open access by DigitalCommons@UTEP. It has been accepted for inclusion in Open Access Theses & Dissertations by an authorized administrator of DigitalCommons@UTEP. For more information, please contact lweber@utep.edu.

AN APPROACH TO POWER EFFICIENCY DETERMINATION IN THE SOLAR
ENERGY SYSTEMS USING CENTRAL COMPOSITE DESIGN AND BOX-BEHNKEN
DESIGN

JUAN VENEGAS MENDEZ

Department of Industrial, Manufacturing & Systems Engineering

APPROVED:

Tzu-Liang (Bill) Tseng, Ph.D., CMfgE

Luis Rene Contreras, Ph.D.

Jaime Sanchez, Ph.D.

Benjamin C. Flores, Ph.D.
Dean of the Graduate School

Copyright ©
By
Juan Venegas Mendez
2013

In dedication to my parents, for all their support, example and love

AN APPROACH TO POWER EFFICIENCY DETERMINATION IN THE SOLAR
ENERGY SYSTEMS USING CENTRAL COMPOSITE DESIGN AND BOX-BEHNKEN
DESIGN

by

JUAN VENEGAS MENDEZ

THESIS

Presented to the Faculty of the Graduate School of

The University of Texas at El Paso

in Partial Fulfillment

of the Requirements

for the Degree of

Master of Science

Department of Industrial, Manufacturing & Systems Engineering

THE UNIVERSITY OF TEXAS AT EL PASO

August 2013

ABSTRACT

We are living in an industrialized world that relies on fossil fuels. The ways, in which these fossil fuels have damaged the earth, in special the environment is worth of special attention and corrective actions. In our days, the climate change (global warming) it is becoming the number one topic. These changes are affecting our health, comfort and our way of living. Solar systems have been working among us since several years, but the truth is that most of us really don't understand how they work and more important, how they work in time in different conditions. Solar panels are one of the most promising renewable energy ways to handle electrification requirements off several isolated consumers worldwide.

Because of this, it was clear which way to take. The main focus of this research is the study of solar panels; watch their behavior on different conditions to determine on which ones this kind of systems can give us more output power. The variables to deal with are going to be the temperature, the angle of the light and the color temperature of the light, all this occurs on a controlled environment following two different methods to analyze the collected data. As objectives, three different point were stated. To find out if all the variables affect our system, which one is the most significant adobe the other for this particular study and to demonstrate the importance of the color temperature of the light on solar panels electricity production.

TABLE OF CONTENTS

	Page
ACKNOWLEDGMENTS	iii
ABSTRACT	v
TABLE OF CONTENTS	vi
LIST OF TABLES	viii
LIST OF FIGURES	ix
CHAPTER	
1. INTRODUCTION	1
1.1 Problem	1
1.2 Objective	1
1.3 Contributions	2
1.4 Motivation	2
1.5 Limitations	3
2. LITERATURE REVIEW	4
2.1 Types of energy	4
2.2 Insolation	7
2.3 Silicon, base for solar cells	8
2.4 Solar cells	12
2.5 How solar cells work	16
2.6 Photovoltaic panels	18
2.7 Different uses for solar panels	20
2.8 Response Surface Designs	23
2.9 First order and second order designs	27
2.10 Central Composite Design	30
2.11 Box-Behnken Design	32
3. METHODOLOGY	34
4. CASE OF STUDY	41
5. DISSCUSIONS AND CONCLUSIONS	49
LIST OF REFERENCES	51

APPENDIX

Appendix A	CCD complete results set	53
Appendix B	BBD complete results set	59
Appendix C	Pictures of the experiment	68
CURRICULUM VITA	73

LIST OF TABLES

	Page
Table 1 Power obtained by origin, solar, lunar and terrestrial	5
Table 2 Sun energy over different spectral regions	6
Table 3 D- and G-Efficiencies of a CCD on a Hypercube	30
Table 4 Table of levels and factors for the experiment	36
Table 5 Central composite and Box-Behnken design parameters	37
Table 6 CCD Design Matrix	38
Table 7 Box-Behnken design matrix	39
Table 8 Table of tools and equipment used with descriptions	40
Table 9 Central Composite Design results table	43
Table 10 Box-Behnken Design results table	44
Table 11 Regression Coefficients for Power from CCD	46
Table 12 Regression Coefficients for Power from BBD	46
Table 13 Table of results for the 3 confirmatory runs	47

LIST OF FIGURES

	Page
Figure 1 Conversion of solar radiation energy on the Earth	5
Figure 2 Color temperature in the Kelvin scale	7
Figure 3 Silicon atom representation	8
Figure 4 Silicon Kernel representation	9
Figure 5 Silicon covalent bond representation	9
Figure 6 Representation of the silicon-bonded structure	10
Figure 7 Supply chain for solar cell modules	13
Figure 8 Production of highly pure TCS from MG-Si	14
Figure 9 Illustration showing the structure of a solar cell with its different layers	15
Figure 10 Image of a solar cell, wire and battery representation of a solar panel	17
Figure 11 Representation of the solar cell replacing a battery in a simple circuit	17
Figure 12 Solar panels array	18
Figure 13 Basic solar system representation	19
Figure 14 Solar array installation in Monterey County	21
Figure 15 Largest solar energy project in the Mojave Desert	23
Figure 16 Central composite design graphic representation	31
Figure 17 The cube for BBD representation	32
Figure 18 2^2 interlocking factorial design	33
Figure 19 Right view of the panel angle and light incidence angle	35
Figure 20 Experiment schematic representation	35
Figure 21 Circuit diagram representation	36
Figure 22 Chart of Temperature vs. Power over time	42
Figure 23 CCD response surface plot	45
Figure 24 BBD response surface plot	45
Figure 25 Response surface optimization plot	48
Figure 26 Chart showing comparison between two types of panels	48

CHAPTER 1

INTRODUCTION

This work presents a study and experiments on how the solar panels behave on different conditions later described, information regarding the production of a solar cell and how a complete arrangement of solar panels are conform to be an electric solar system. The experiment was conducted following central composite design and Box-Behnken methodologies to determine the optimal conditions for the solar panels to work. Both methodologies are Response Surface techniques under the design of experiments area. Three factors were analyzed and studied, Temperature, Angle and color temperature of light.

1.1 Problem

The problem that this thesis discusses is the gap of information from the solar panels manufacturers in which describes the behavior of the solar panels on different conditions. All the solar panels come only with the testing information at standard testing conditions, this is, direct sunlight (light hitting directly to the panel) at 25°C.

Another problem is that the information on how the panels behave with different light color temperature is very limited. Finally, the difference on power output efficiency between a monocrystalline and a polycrystalline panel, the price gap is big, but how big is the difference on efficiencies.

1.2 Objective

To find how different conditions can affect the output power on a solar panel electricity production, finding which factor is more significant than the others. Another one would be not only to find the more significant factor but also to find the optimal conditions

for a solar panel to work at its best possible performance. Another purpose may be to detect an opportunity area for a new development that can improve the performance of the panels.

1.3 Contributions

This work presents a statement on how to increase the output power on a solar energy system. Second, it compares the advantage of using a mono-crystalline or polycrystalline photovoltaic panel, which one is more efficient knowing that in general terms the monocrystalline panels are more expensive than the polycrystalline ones, taking in count the same characteristics in average.

Third, one of the main contributions was finding out that the color temperature of the light affects a lot the output power of the solar panels. Knowing that the sunlight color temperature is 5000K (on the Kelvin scale) and that in fact the color that produces the most power from the panel is 3000K or lower.

1.4 Motivation

One of the motivations for performing this research was the fact that these days, global warming and resource depletion are really affecting us in a lot of ways, and if this paper could, one way or another, help a little bit people to understand better another ways to cover their energy necessities, in this case the use of solar panels would be a nice contribution. The reality is that it could be any renewable energy system device; the main objective with this study will be trying to change and improve the way we use our resources, making them more environmentally friendly.

Second thing is that in the reality there are not too many studies like this one, and the ones out there do not give the whole picture of it, so this provides useful information that

can help decision making on this field. Finally, because the potential and freedom that can be achieved by using renewable energy sources will lead to a better global community, society and quality of life.

1.5 Limitations constraints

Some of the limitations founded performing this research and the experiment were the lack of tools and equipment at the time of the experiment, for example, a watt-meter was missing and instead of this a regular multimeter was used, this caused that at the time of measuring the output for each replicate on each event first the voltage was recorded then the current and then applying the ohms law the power in watts was calculated. Also, the equipment to maintain and control the environment was not very precise so it takes more time to control the temperatures and perform the experiment.

Another one is that it was hard to find information on how the solar panels behave on different temperatures, some database of another experiments conducted and other experiments that includes different factors than temperature, humidity or angle. One more limitation was the lack of information regarding the behavior of the silicon with different color temperatures. It was intended to include a section talking about this and with this complement the conclusion regarding the results obtained with this factor.

CHAPTER 2

LITERATURE REVIEW

The main focus of this thesis is the solar panel, but what is a solar panel? What components conform a solar panel? Well, a solar panel has many components like glass, aluminum for the frame, some plastic parts and other materials for joining everything together, but the core of the solar panel are the solar cells. What are the solar cells? How do they work? What are they made of? This work describes all this on the next chapter, but first it is important to understand that the main objective of the solar panels is the generation of electricity, so let's see what is energy first, in fact the focus will be renewable energy.

Renewable energy has had several definitions over the last 50 years. *"A broad definition from the environmental movement since the 1960s includes any energy source that is alternative to conventional fossil fuels."*[1] This definition takes in count geothermal energy, which is not really a renewable resource because the time that it is needed for the earth to store the heat is too much, indeed it requires hundreds of thousands of years to replace the heat extracted from the geothermal deposit till it generates a new deposit.

2.1 Types of energy

Primordial: These are the sources that were originated with the formation of the earth.

Fossil: This is decayed organic (carbon-containing) matter fossilized over millions of years that can be extracted by the mineral extraction industries.

Renewable: This consists of the energy fluxes available on a daily basis from incoming solar and lunar sources. Energy available for the humans also can be classified by origin. This is solar, lunar, and terrestrial. [1] The power obtained is as follows:

Table 1 - Power obtained by origin, solar, lunar and terrestrial [1] [2]

Solar	Thermal (heat and radiation)	76 PW
	Hydropower (the hydrologic cycle)	40 PW
	Kinetic (wind power)	0.37 PW
	Biomass (for food and power)	0.04 PW
Lunar	Tidal (coastal water and wave power)	0.003 PW
Terrestrial	Geothermal heat (estimated resource)	0.11 PW

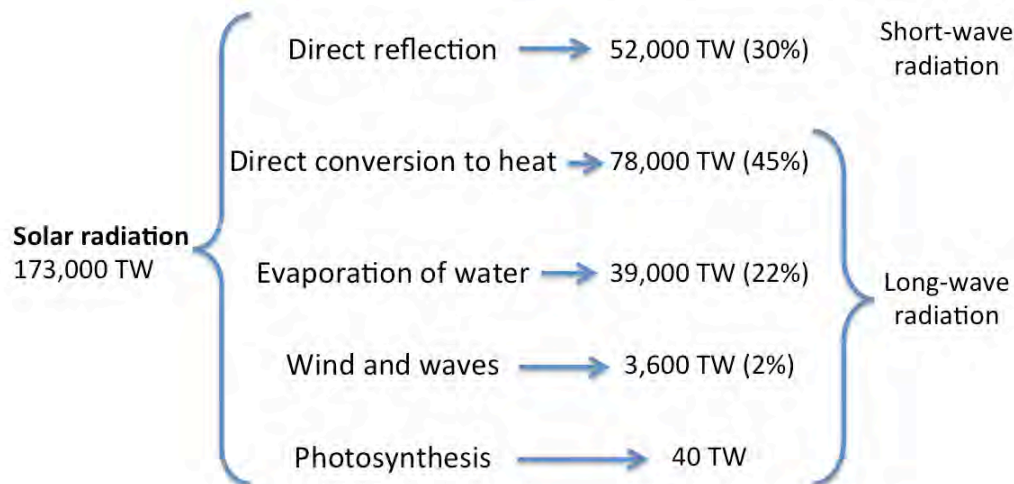


Figure 1 – Conversion of solar radiation energy on the Earth [3]

“If we could extract more energy from the sun and other renewable energies, we would be able to satisfy the whole world electricity consumption. In 2008, *total worldwide electricity generation* was 72.73 EJ or 20.20 petawatts (2.02×10^{16} W).” [2] The potential extraction of renewable energy could be: *solar energy* 1600 EJ (444,000 TW/h), *wind power* 600 EJ (167,000 TW/h), *geothermal energy* 500 EJ (139,000 TW/h), *biomass* 250 EJ (70,000 TW/h), *hydropower* 50 EJ (14,000 TW/h) and *ocean energy* 1 EJ (280 TW/h). [4]

Energy can be utilized but not consumed. It is a law of nature that energy is conserved. All energy we use is degraded into heat and eventually radiated out into space. The consumable is not energy; the consumable is the fact that energy has not been yet randomized. The sun radiates in all regions of the spectrum, from radio waves to gamma rays. Our eyes are sensitive to less than one octave of this, from 400 to 750 THz (750 to 400 nm), are you known, for obvious reasons, as visible. Although narrow, it contains about 45% of all radiated energy.

At the distance of one astronomical unit, the power density of all of the solar radiation is about 1360 W per square meter, a value called solar constant, which is not really constant, it varies a little throughout the year, being largest in January when the Earth is nearest the sun. The expression power density is used to indicate the number of watts per square meter. This is also known as energy flux. [3]

Roughly, the distribution of energy over different spectral regions is:

Table 2- Sun energy over different spectral regions [3]

Infrared and below	($f < 400$ THz, $\lambda > 750$ nm)	46.3%
Visible	($f < 750$ THz, 400 nm $< \lambda < 750$ nm)	44.6%
Ultraviolet and above	($f > 750$ THz, $\lambda < 400$ nm)	9.1%

Under the visible spectral region, the light has different colors or temperatures, this are measured in Kelvin°. Fig. 2 shows the different colors or temperatures for the light.

Color Temperatures in the Kelvin Scale

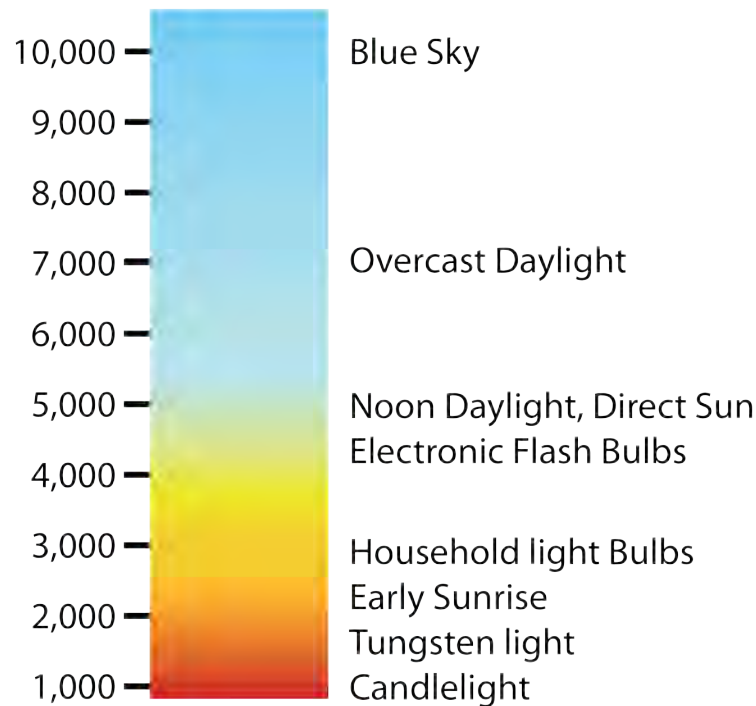


Figure 2 – Color temperature in the Kelvin scale

2.2 Insolation

Insolation is the power density of the solar radiation. It is known that the insolation on a surface that faces the sun and is just outside Earth's atmosphere is called solar constant. It has a value of 1360 W/m^2 . It is also convenient to define a solar surface constant that is a value of insolation on a surface that at sea level faces the vertical sun on a clear day. This constant has the convenient value of about 1000 W/m^2 (1 kW/m^2) or "one sun".

The position of the sun is characterized by the zenith angle, X (the angle between the local vertical and the line from the observer to the sun), and by the azimuth, x , measured clockwise from the north. A Geocentric system has its origin at the center of the earth while a heliocentric system has its origin at the sun.

In the topo-centric system, both X and x are functions of:

- The local time of day, t
- The day of the year, d
- The latitude of the observer, l

Now that the general concepts of energy were covered, more concretely renewable energy, it is needed to understand how a solar panel work, and for that we need to know how a solar panel is conformed of. Let's understand first the core of a solar panel, the solar cell. [1]

2.3 Silicon, base for solar cells

A silicon atom consists of a nucleus (dark sphere), containing 14 protons (circles with "+" sign) and 14 neutrons (solid circles), surrounded by 14 electrons (circles with "-" sign). The nucleus carries a charge of +14 but the atom (unless it is ionized) has no net charge owing to the 14 electrons swarming around it.

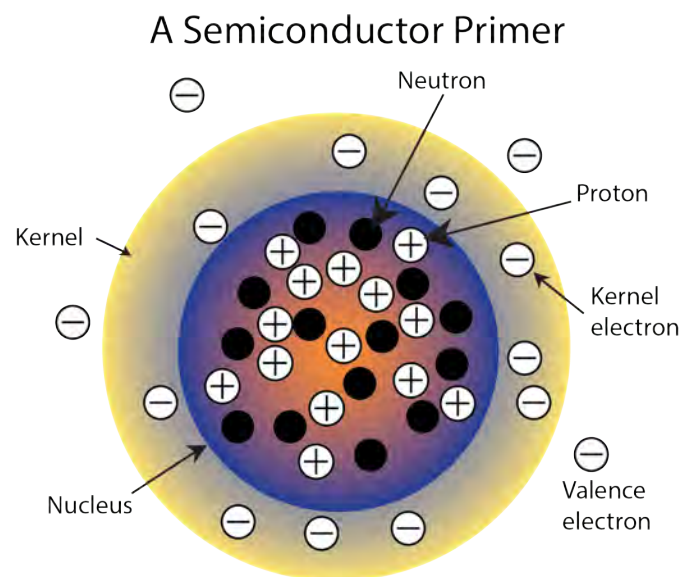


Figure 3 – Silicon atom representation

Observe that 10 of the 14 electrons are tightly bound to the nucleus and are difficult to remove. However, four electrons (called valence electrons) can be easily removed (ionizing the atom) and are, therefore, able to take part in chemical reactions. Silicon is, consequently tetravalent. It proves convenient to represent a silicon atom as consisting of a kernel surrounded by four valence electrons. [3] Two silicon atoms can be bound one to another by exchanging valence electrons. Such a bond is called a covalent bond. Because it has four valence electrons, each silicon atom can make four covalent bonds attaching itself to four neighboring atoms. This might lead to a lattice structure as depicted below.

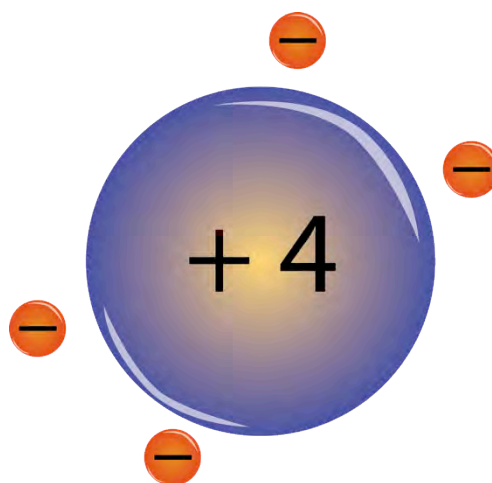


Figure 4 - Silicon Kernel representation

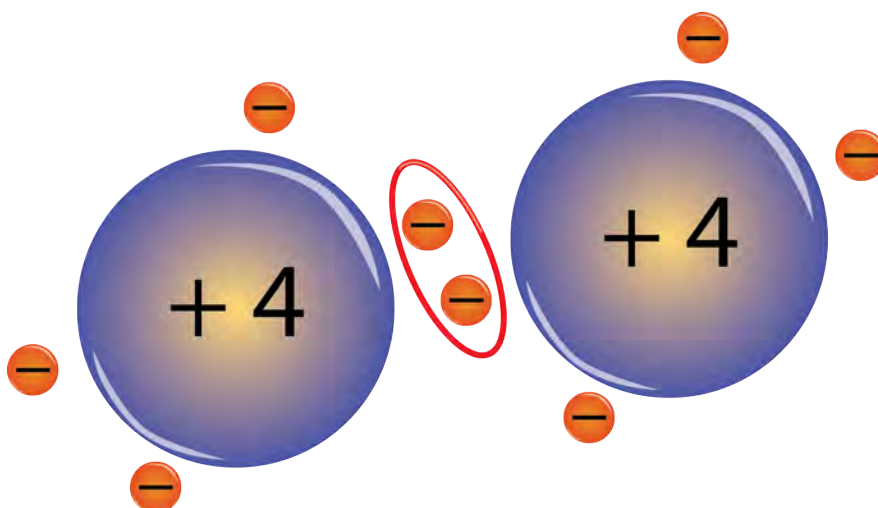


Figure 5 - Silicon covalent bond representation

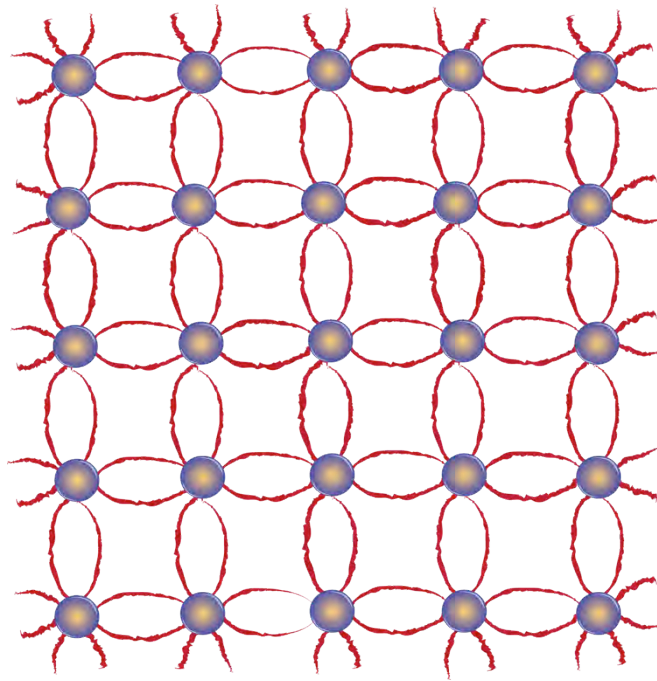


Figure 6 – Representation of the silicon-bonded structure

At 0 K, all valence electrons are engaged in covalent bonds and are, therefore, unavailable as carriers, that is as transporters of electric charge. No current can flow through the crystal because it is an insulator. However, if a bond is disrupted (by thermal agitation of the lattice or through the impact of a photon or a high speed electron), then one of the valence electrons is ejected from the bond and becomes free to carry electricity, leaving behind an incomplete bond, one in which a hole exists into which an electron from a neighboring bond can fall. This causes the hole to move to a new place. Thus the disruption of a bond creates a pair of carriers, an electron and a hole imparting some degree of conductivity to the material. It is clear, that in this particular case, the number of free (conduction) electrons is exactly equal to the number of holes. Such materials are called intrinsic. From this we know that semiconductors have an electric conductivity that

increases when the temperature increases: the warmer the material the greater the number of carriers.

So far the literature has deal with absolutely pure silicon. In fact, all silicon contains some impurity, which may dramatically alter the properties of the material. Since phosphorus has a valence of 5, it has enough electrons to complete the four covalent bonds that anchor the atom in the lattice. In addition, there is one electron left over, which then acts as a carrier, the material is ***n-silicon***, one in which the dominant carrier is negative. The phosphorus kernel has a +5 charge and the crystal site has only 4 covalent bond electrons. Thus, the site has a +1 positive charge, which being immobile does not constitute a carrier. It is called a ***donor***.

If instead of a pentavalent atom such as phosphorus, the impurity is a trivalent one such as aluminum or boron, then there is an insufficiency of electrons and only three of the covalent bonds are satisfied, leaving one incomplete, that is, leaving a free hole, the material is ***p-silicon***, one in which the dominant carrier is a positive hole. Similarly to the case of phosphorus the aluminum atom represents a -1 immobile charge, it is an ***acceptor***. The introduction of certain impurities into the mass of silicon is called ***doping***. Typically, the amount of doping is small, ranging from 1 dopant atom for every 10 thousand silicon atoms (extremely heavy doping) to 1 dopant atom for every 100 million silicon atoms (very light doping). Things start becoming really interesting when a crystal has a p-region juxtaposed to an n-region.

Electrons, more abundant in the n-side, tend to diffuse to the p-side, while holes tend to diffuse into the n-side. The donors and acceptors, of course, cannot move. The net effect of these diffusions is that the n-side becomes positive. By the same token, the p-side

becomes negative. Thus a contact potential is created, which in silicon at room temperature can be around 1 V, depending on the doping.

The potential across most of the n-side and p-side of the device is constant (no electric field). The entire field is concentrated across a narrow transition region. Owing to the narrowness of this region (a few tens of a nanometer), the electric fields developed can be enormous, up to tens of millions of volts/meter.

When light shines near a p-n junction, electron-hole pair may be created on either side. If they are very far from the transition region, they will recombine after a few microseconds. If however, they are near, they may drift toward the region of high electric field. In this case, an electron created in the p-side may fall into the n-side, while a hole created on the n-side may fall to the p-side. In either case, these charges counteract the contact potential. Thus, the effect of light on a p-n junction is the lowering of the contact potential. After understanding how doped silicon can produce renewable energy we are going to see one way of how solar cells are been manufactured [3].

2.4 Solar cells

Building a solar cell

The production of a typical silicon solar cell (Fig. 7) starts with the carbo-thermic reduction of silicates in an electric arc furnace. In this process large amounts of electrical energy break the silicon–oxygen bond in SiO_2 via an endothermic reaction with carbon. Molten Si-metal with entrained impurities is withdrawn from the bottom of the furnace while CO_2 and fine SiO_2 particles escape with the flu-gas. Metallurgical grade silicon (MG-Si) at about 98.5% purity is sold to many different markets. The majority of MG-Si is used for silicones and aluminum alloys.

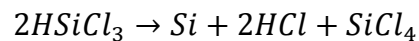
A small but rapidly growing portion is used for solar applications. [5] Highly pure poly-silicon suitable for solar cells and microelectronics is typically produced in two steps. In the first step, MG-Si reacts with HCl to form a range of chlorosilanes, including tri-chlorosilane (TCS). TCS has normal boiling point of 31.8°C so that it can be purified by distillation. (Fig.8)



Figure 7 – Supply chain for solar cell modules

Poly-silicon is most often produced in the same manufacturing facility by pyrolysis of TCS in reactors that are commonly called Bell or Siemens reactors. [5]

In the Bell reactor, TCS passes over high purity silicon starter rods, which are heated to about 1150°C by electrical resistive heating. The gas decomposes as:



Equation 1 – Tri-chlorosilane decomposition formula

Silicon deposits on the silicon rods as in a chemical vapor deposition process. 9N (99.999999999%) silicon is used for microelectronics applications. Silicon that is 6 N or better is called solar grade silicon (SOG-Si) and it can be used to produce high quality solar cells. The total process therefore takes silicon at low purity and converts it to poly-silicon at high purity. In the next step, it is necessary to produce thin wafers of silicon. They typically have a thickness of 200–350 mm and a resistivity of about 1 W/cm. The recent industry trend has been towards thinner wafers and new wafer saws are capable of producing wafers with a thickness of 180 mm. Thin wafers are advantageous since the

material requirements are small, but they cannot be too thin since they are very brittle and difficult to process.

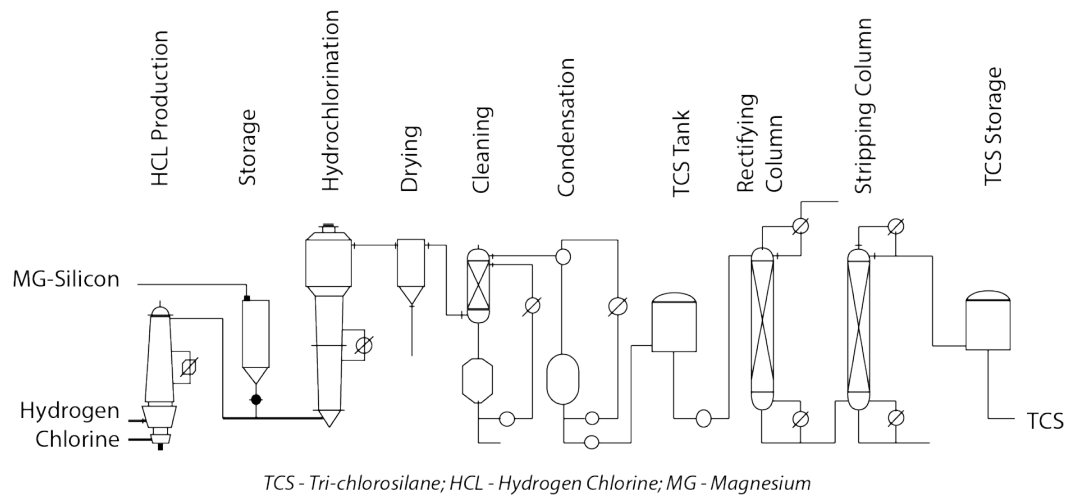


Figure 8 – Production of highly pure TCS from MG-Si

The most widely used wafering process consists of melting and re-solidifying pure silicon. These silicon ingots are then cut to form wafers as in the microelectronics industry. It may take two days or more to produce a single silicon ingot. One major disadvantage of both the CZ and Bridgman processes is that the silicon blocks must be cut using wired saws to produce thin wafers. The wires used in the sawing process may be as thick as the wafers themselves and 50% or more of the material is therefore lost as dust or must be recycled at significant cost. Many processes have therefore been proposed to achieve wafering and crystallization in one continuous step. None of these have yet had a significant impact on industrial wafer production.

Solar cells are produced from silicon wafers in a sequence of steps. The wafers are first treated with chemicals to enhance optical and electrical properties. Silicon, a group 4 element, is doped with the neighboring group 3 and 5 elements, typically boron and

phosphorous, to produce the p-n junction with associated surplus and deficiency of electrons in the conduction bands.

Anti-reflection coating layers reduce reflection losses at the front surface by trapping incident light within the cell. Front and back electrical contacts are added to complete the solar cell. Individual cells are finally integrated into panels and festooned with inverters and other systems to produce electricity matched to the end user's requirements. [5] Now that it is known how silicon can be used for energy transformation from solar radiation to electricity and also how solar cells are made, so let's now put all that information directly into a solar cell.

Structure of a solar cell.

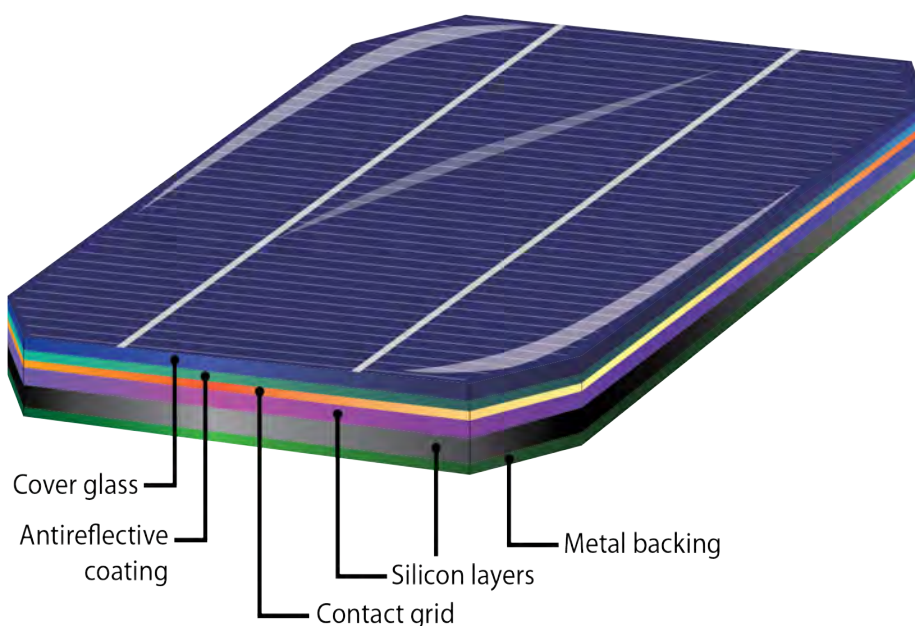


Figure 9 – Illustration showing the structure of a solar cell with its different layers

2.5 How solar cells work

The solar cell is the basic building block of solar photovoltaics. The cell can be considered as a two terminal device, which conducts like a diode in the dark and generates a photo-voltage when charged by the sun. Usually it is a thin slice of semiconductor material of around 100 cm² in area. The surface is treated to reflect as little visible light as possible and appears dark blue or black. [6]

A pattern of metal contacts is imprinted on the surface to make electrical contact (Fig. 10(a)). When charged by the sun, this basic unit generates a dc photo-voltage of 0.5 to 1 volt and, in short circuit, a photocurrent of some tens of milliamps per cm². Although the current is reasonable, the voltage is too small for most applications.

To produce useful dc voltages, the cells are connected together in series and encapsulated into modules. A module typically contains 28 to 36 cells in series, to generate a dc output voltage of 12 V in standard illumination conditions (Fig. 10(b)). The 12 V modules can be used singly, or connected in parallel and series into an array with a larger current and voltage output, according to the power demanded by the application. (Fig. 10(c)). [6]

The solar cell can take the place of a battery in a simple electric circuit (Fig. 11). In the dark the cell in circuit (a) does nothing. When it is switched on by light it develops a voltage, or E.M.F. (electro-motive force), analogous to the E.M.F. of the battery in circuit (b). The voltage developed when the terminals are isolated (infinite load resistance) is called the open circuit voltage V_{oc} . The current drawn when the terminals are connected together is the short circuit current I_{sc} .

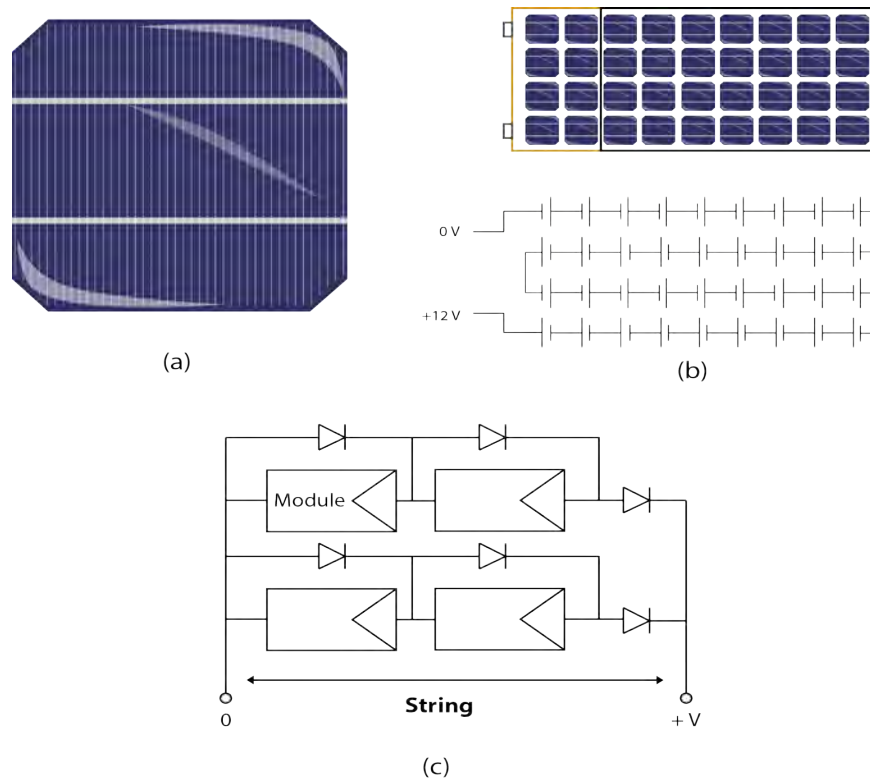


Figure 10 - Image of a solar cell, wire and battery representation of a solar panel, and wire representation of a solar panel system

For any intermediate load resistance R_L the cell develops a voltage V between 0 and V_{oc} and delivers a current I such that $V = IR_L$ and $I(V)$ is determined by the current voltage characteristic of the cell under that illumination. The illumination as well as the load determines both, I and V . [6] Now that we understand how a solar cell is made and how it works, let's get into a solar panel.

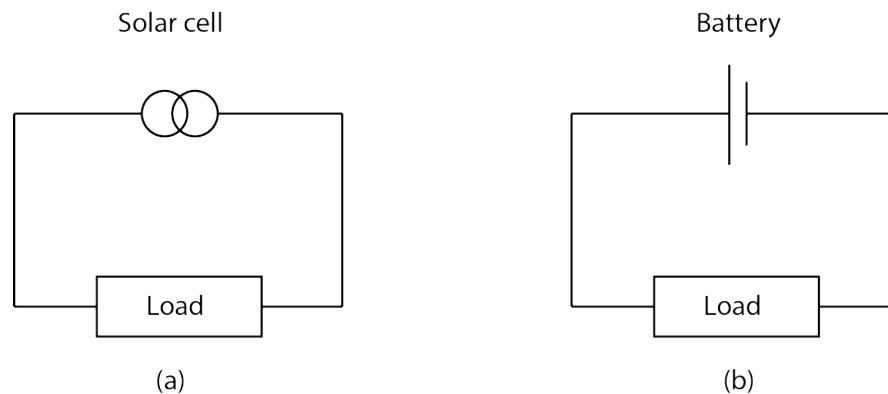


Figure 11 - Representation of the solar cell replacing a battery in a simple circuit

2.6 Photovoltaic panels

The previous section mention that a solar panel is nothing more than a series of solar cells connected in such a way that we can effectively use the electricity, encapsulated into some layer of glass and other materials, this with the intention of protecting the solar cells, that are the core of the solar panel.

Photovoltaic panels have low operating cost, since they consume no fuel; their peak power can by only realized on a clear day, with the converter facing the sun. The average power will be less than half the peak power for sun tracking systems (owing to nighttime) and less than one-fourth of peak power for non-tracking systems. [3] The efficiency of photovoltaic systems may be over 20% for sophisticated crystalline silicon systems and some 5% for some inexpensive thin film ones. However, efficiency is not of primary interest in many photovoltaic installations. The cost per peak watt may be the important characteristic. [3]

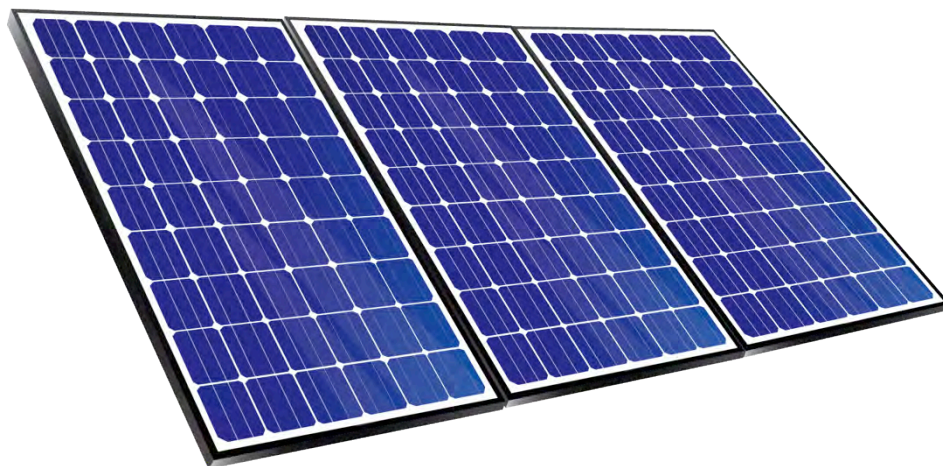


Figure 12 – Solar panels array

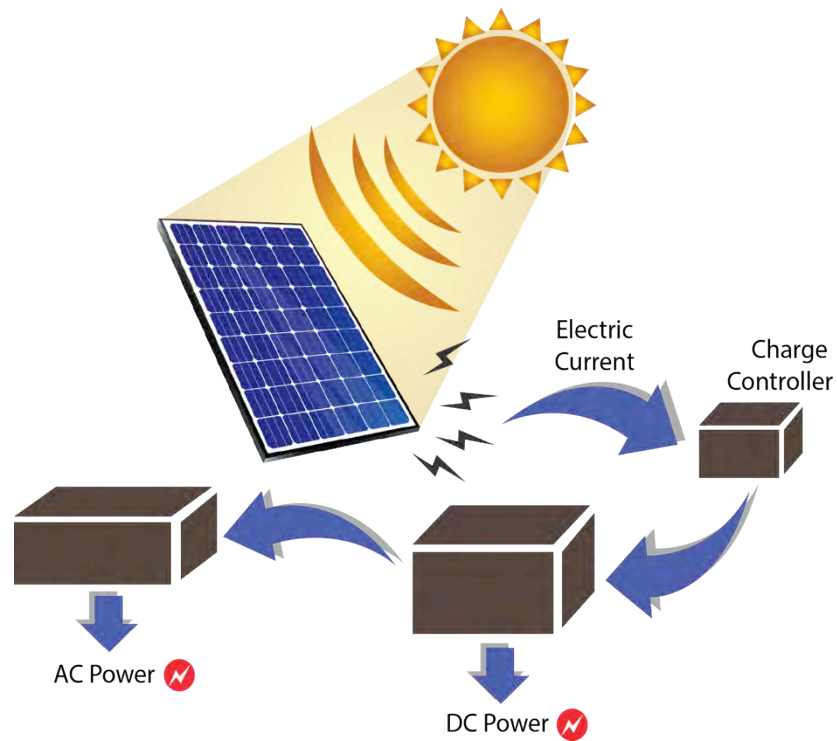


Figure 13 – Basic solar system representation

If the building is off-grid, as some rural properties are, that is, if it has to be entirely self-sufficient, expensive batteries or some other storage scheme is needed. On the other hand, if the building is connected to the power grid, the local utility company in what it is called a utility-tie system can provide storage. The excess of energy generated by the consumer can be sold at the utility for a price below that charged by the utility to the customer.

The price differential would pay for the storage and distribution. A dual metering system can be used; one meter measures the outgoing power from the customer to the utility and the other the power from the utility to the customer. A utility-intertied inverter must be used so that the frequency and the phase of the customer-generated electricity match the grid. In areas of unreliable energy supply, subjected to frequent blackouts, a hybrid system of the off-grid and the utility-tie system may be useful. [2] Such building-

integrated photovoltaic (BIPV) systems will become progressively more popular as the price of solar panels decreases. [3]

Broadly, three distinct techniques are used in building solar cells:

- Crystalline material, most frequently silicon. These are expensive to produce but yield good efficiencies (>20%) if they are made of single crystals. Somewhat cheaper, but less efficient, are polycrystalline units.
- Amorphous thin films (Si, GaAs, CuInSe₂, TiO₂, etc.) have efficiencies of some 7% but are much less expensive. They can be made into flexible sheets.

Organic polymers, still in early development, could easily become the best overall solution. They promise to be low cost, lightweight, and flexible. One can imagine photovoltaic blankets cheap enough to serve as roofing materials replacing present day shingles, tarpaper or tiles. Manufacturing methods will probably be less toxic than those of inorganic materials. [3]

2.7 Different uses for solar panels

Solar panels have a wide variety of uses. Here we can see an example of what we can do with them. From a distance, the new structure at Monterey County's Laurel Yard Complex in Salinas, California, looks like an ordinary parking lot canopy. But a closer inspection shows it is actually an impressive array of solar panels that is expected to save the county thousands of dollars a year in energy costs.

Monterey County's new 141 kilowatt solar photovoltaic (PV) energy system has the capacity to convert sunlight into 192,000 kilowatt hours of energy per year, an energy output equivalent of more than 15,000 gallons of gas or 1,150 60-watt light bulbs. The system generates enough energy to power all eight public works facilities and offices at the

county-owned Laurel Yard Complex for six months out of the year, effectively cutting annual power bills in half.



Figure 14 – Solar array installation in Monterey County (Picture from energy.gov)

The new solar array is expected to save the county an estimated \$222,000 in energy costs during its first five years of operation and at least \$18,800 per year starting during year six of operation. Additionally, the system is expected to decrease carbon dioxide emissions by at least 270,000 pounds each year. The county completed the project with assistance from the Energy Department’s Energy Efficiency and Conservation Block Grant Program. [7]

Interesting things to know about solar energy

Solar energy is the most abundant energy resource on earth – 173,000 terawatts of solar energy strikes the Earth continuously. That’s more than 10,000 times the world’s total energy use.

Bell Laboratories built the first silicon solar cell, the precursor of all solar-powered devices, in 1954. On page one of its April 26, 1954 issue, The New York Times proclaimed the milestone, “the beginning of a new era, leading eventually to the realization of one of

mankind's most cherished dreams, the harnessing of the almost limitless energy of the sun for the uses of civilization."

The space industry was an early adopter of solar technology. In the 1960s the space industry began to use solar technology to provide power aboard spacecraft's. The Vanguard 1, the first artificial earth satellite powered by solar cells, remains the oldest manmade satellite in orbit – logging more than 6 billion miles.

Fast track to today and demand for solar in the United States is at an all-time high. In the first quarter of 2012, developers installed 85 percent more solar panels compared to the first quarter of last year. Total U.S. installations may reach 3,300 megawatts this year – putting the country on track to be the fourth largest solar market in the world.

As prices continue to fall, solar energy is increasingly becoming an economical energy choice for American homeowners and businesses. Still, the biggest hurdle to affordable solar energy remains the soft costs – like permitting, zoning, and hooking a solar system up to the power grid. On average local permitting and inspection processes add more than \$2,500 to the total cost of a solar energy system. The Energy Department SunShot Initiative works to aggressively drive down these soft costs – making it faster and cheaper for families and businesses to go solar.

In California's Mojave Desert, the largest solar energy project in the world is currently under construction. The project relies on a technology known as solar thermal energy. Once the project is complete 350,000 mirrors will reflect light onto boilers. When the water boils, the steam turns a turbine, creating electricity. The project is expected to provide clean, renewable energy for 140,000 homes and is supported by an Energy Department loan guarantee.



Figure 15 - Largest solar energy project in the Mojave Desert (Picture from energy.gov)

Now it is known how solar panels work and in the last section 2 examples of how solar panels are being used in different ways and scales were described. Now, for main purposes of this study is needed to understand some basic statistical concepts as well as the basic approaches of DOE (Design of experiments) that are going to be used. [7]

2.8 Response Surface Designs

The only objective of an experimental design is to discover the best treatment between all the other ones tested but a response surface design pretends to find the optimal conditions of a certain process. Because of this it presents a more difficult challenge for a researcher and requires a more complete strategy because the possibility of performing several sequential experiments and advanced mathematical techniques are an option.

The response surface methodology or RSM study the relationship between several input variables and one or more response variable. Box and Wilson introduced the method in 1951. The objective of the RSM is to take hand on several designed experiments to obtain an optimal response. The response variable that we may be looking could be y and it has a set of predictor variables X_1, X_2, X_k . For some procedures, based on the fundamental engineering, chemical or physical principles, the nature of the relationship between y and the x 's might be known exactly.

It is consider the most common scenario where the underlying mechanism is not fully understood, and the experimenter must estimate the unknown function g with an appropriate empirical model $y = f(X_1, X_2, ..., X_k) + \varepsilon$. Usually the function f is a first order or second order polynomial. This empirical model is called a response surface model. Response surface methodology (RMS) is a compilation of statistical and mathematical techniques for developing, refining and optimizing processes.

The most used application of RSM is in the industrial world, particularly in circumstances where several input variables potentially influence some performance measure or quality characteristic of the product or process. This performance measure or quality characteristic is called the response. It is usually measured on a continuous scale, although attribute responses, ranks, and sensory responses are not usual. The input variables are sometimes called independent variables, and they are subject to the control of the engineer or scientist, at least for testing and experimenting purposes. [9]

Response surface methodology (RMS) is a set of techniques that encompasses, setting up a series of experiments that will yield adequate and reliable measurements of the response of interest, also fitting a mathematical model that best fits the data collected

from the design chosen and by conducting appropriate tests of hypotheses concerning the models parameters and finally to set up the optimal settings of the experimental factors that produce the maximum or minimum value of response. If getting the best value of the response is beyond the available resources of the experiment, then response surface methods are aimed to obtain at least a better understanding of the overall system. When certain laws that lead to a deterministic relationship between the response and the set of experimental factors chosen control the behavior of the measured response of interest, it should then be possible to determine the best conditions of the factors to optimize a desired output. [10]

In any system in which variable quantities change, the interest might be assessing the effects of the factors on the behavior of some measurable quantity. Such an assessment is possible through regression analysis. Using data collected from a set of experimental trials, regression helps to establish empirically the type of relationship that is present between the response variable and its influence factors. The response variable is the dependent variable and is called response and the levels of influencing factors are called regressor or input variables.

Regression analysis is one of the most used tools of cause and effect relationships. As mentioned before, a response surface method is a supplementary technique employed before while and after a regression analysis is performed on the data. Previous the regression analysis, the experiment must be designed, that is, the input variables must be selected and their values during the actual experimentation designated. Once the regression analysis is performed, certain model testing procedures and optimization techniques are applied. Consequently, subject of RSM includes the application of regression

as well as other techniques in an effort to gain a better understanding of the characteristics of the response system being study. [10]

Factors are inputs variables or conditions whose values or settings can be controlled by the experimenter. Likely, if the experimenter changes the settings of at least one factor, the value of the response variable varies as well. The factors on a regression analysis can be qualitative or quantitative. If there are qualitative factors in the experiment, they are considered blocking variables. The specific factors whose levels are to be studied in detail are those that are quantitative in nature, and their levels are assumed to be controlled without margin to mistakes by the experimenter.

The response variable is the measured quantity whose value is assumed to be affected by changing the levels of the factors. The true value of the response given any particular combination of factor levels and without experimental error of any kind is denoted by η . When we say that the value of the response surface η depends upon the levels X_1, X_2, \dots, X_k , the value of which for any given value of η , that is, the combination that the factor levels supply to the corresponding value of η , that is:

$$\eta = \phi(X_1, X_2, \dots, X_k)$$

Equation 2 – True response surface function

The function ϕ is called the true response surface function and is assumed to be a continuous function of the X_i . [10] In general the steps to apply a RSM are the following:

First, determine the natural variables (X_j). For this purpose it is important to determine the levels of these variables and to code them. The coded variables give a better comparison between them; it is also recommended that the coding must be equidistant.

Second, solve the model; check the normality and the variance. Third, get the response surface from a second order like a CCD that has the following properties.

- Is orthogonal (Obtains the principal coefficients separate from each other)
- D-Efficiency (maximize the determinant $|X^tX|$ with this the confidence region of the ellipse on which the coefficients are going to be determined)
- G-Efficiency (it obtains the variance from the minimal prediction of the model)
- It is easy to construct this model for rotatability (the variance of the prediction over the sphere has radio 1) when the axial points are added. The number of center point recommended for the experiment to give stability to the prediction variance is 3 to 5 points

Finally, determine the regression equation of second order from the ANOVA table.

2.9 First order and second order designs

A first order model is denoted in Eq. 3, and its orthogonal designs are commonly used for a two-level factorial design, which means each factor has two levels. The total sets will be 2^k plus the center runs, where k denotes the number of factors.

$$\hat{y} = a_0 + \sum_{j=1}^n a_j x_j$$

Equation 2 – equation of a first order model

However the first order design should not only consider the main effects of the factors, but also frequently need to include the interaction items, which would mean the model is then represented as in Eq. 4

$$\hat{y} = a_0 + \sum_{j=1}^n a_j x_j + \sum_{1 \leq i < j} a_{ij} x_i x_j$$

Equation 3 – Equation of a first order model with iterations

The requirements for fitting a second order model are at least three levels of each design variables and at least $1+2k+k(k-1)/2$ distinct design points as shown in Eq. 5. The most popular second order design is the CCD. [11] The objective of a second order experiment is to model the behavior of the process on a specific region relatively small to determine the combination of factors that will give a higher probability of an optimal result.

$$\hat{y} = a_0 + \sum_{j=1}^n a_j x_j + \sum_{1 \leq i < j} a_{ij} x_i x_j + \sum_{j=1}^2 a_{ij} x_j^2$$

Equation 4 – Equation of a second order model

Design of experiments assures the precision and efficiency of the experiments, that's the reason why for this particular study the methodology to follow will be Central Composite Design and Box-Behnken design. Both approaches are included in the DOE and response surfaces methodologies. Lucas (1976) compared the performance of several types of second order designs, like central composite designs, Box-Behnken designs, uniform shell designs, Hoke designs and Box-Draper saturated designs, on the basis of their D- and G-efficiencies. He concluded that all of the compared designs had high efficiencies, and that while more efficient designs were possible, they either remained undiscovered or required significantly more design points.

In a hyper-spherical region of radius one, the study by Lucas (1976) indicates that the three designs; central composite, Box-Behnken and uniform shell; have high D-

efficiency and moderate to high G-efficiency. The uniform shell design however is not as efficient as the other two designs.

D-optimal designs are one form of design provided by a computer algorithm. These types of computer-aided designs are particularly useful when classical designs do not apply. Unlike standard classical designs such as factorials and fractional factorials, D-optimal design matrices are usually not orthogonal and effect estimates are correlated.

These types of designs are always an option regardless of the type of model the experimenter wishes to fit (for example, first order, first order plus some interactions, full quadratic, cubic, etc.) or the objective specified for the experiment (for example, screening, response surface, etc.). D-optimal designs are straight optimizations based on a chosen optimality criterion and the model that will be fit. The reasons for using D-optimal designs instead of standard classical designs generally fall into two categories, standard factorial or fractional factorial designs require too many runs for the amount of resources or time allowed for the experiment or the design space is constrained (the process space contains factor settings that are not feasible or are impossible to run). [12]

From table 3 it is note that the D-efficiency of a CCD is higher for $k \leq 5$ (where the factorial portion consists of a full factorial array) and decreases as the number of factors increases. [13] D-efficiency designs pursues the minimization of $|(X'X)^{-1}|$, or evenly maximize the determinant of the information matrix $X'X$ of the design while the objective of the G-efficiency design is to minimize the maximum entry in the diagonal of the matrix $X(X'X)^{-1}X'$ causing the effect of minimizing the maximum variance of the predicted values.

Table 3 – D- and G-Efficiencies of a CCD on a Hypercube [13]

Number of factors	Number of points	D-Efficiency	G-Efficiency
2	9	0.974	0.828
3	15	0.942	0.836
4	25	0.911	0.780
5	43	0.885	0.602
5c	27 ($I=A_1A_2A_3A_4A_5$)	0.842	0.749
6	77	0.853	0.417
6c	45 ($I=A_1A_2A_3A_4A_5A_6$)	0.852	0.625
6d	29 ($I=A_1A_2A_3=A_4A_5A_6$)	0.485	0.074
7	143	0.813	0.264
7c	79 ($I=A_1A_2A_3A_4A_5A_6A_7$)	0.845	0.442
7d	47 ($I=A_1A_2A_3A_4A_5=A_1A_6A_7$)	0.645	0.108
8	273	0.790	0.155
8c	145 ($I=A_1A_2A_3A_4A_5A_6A_7A_8$)	0.821	0.283
8d	81 ($I=A_1A_2A_3A_4A_5=A_1A_2A_6A_7A_8$)	0.833	0.469

2.10 Central Composite Design

The central composite designs or CCDs were introduced by Box and Wilson (1951) and are without any doubt the most popular class of second order designs and an alternative class of designs to the $3k$ factorial designs. Much of the motivation of the CCD evolves from its use in sequential experimentation. It is a design usually used for building second order models, without applying a complete three level factorial experimental design. CCD contains a fixed two level factorial design and axial points (fig. 16). If there are k factors, the axial number is 2^k .

If the distance from the center of the design space to a factorial point is one unit for each factor, the distance from the center of the design space to the axial point is $\pm\alpha$, which is expressed in the next equation, and $|\alpha|>1$.

$$\alpha = (2^k)^{1/4}$$

Equation 6 – Eq. to calculate the distance between center and axial points

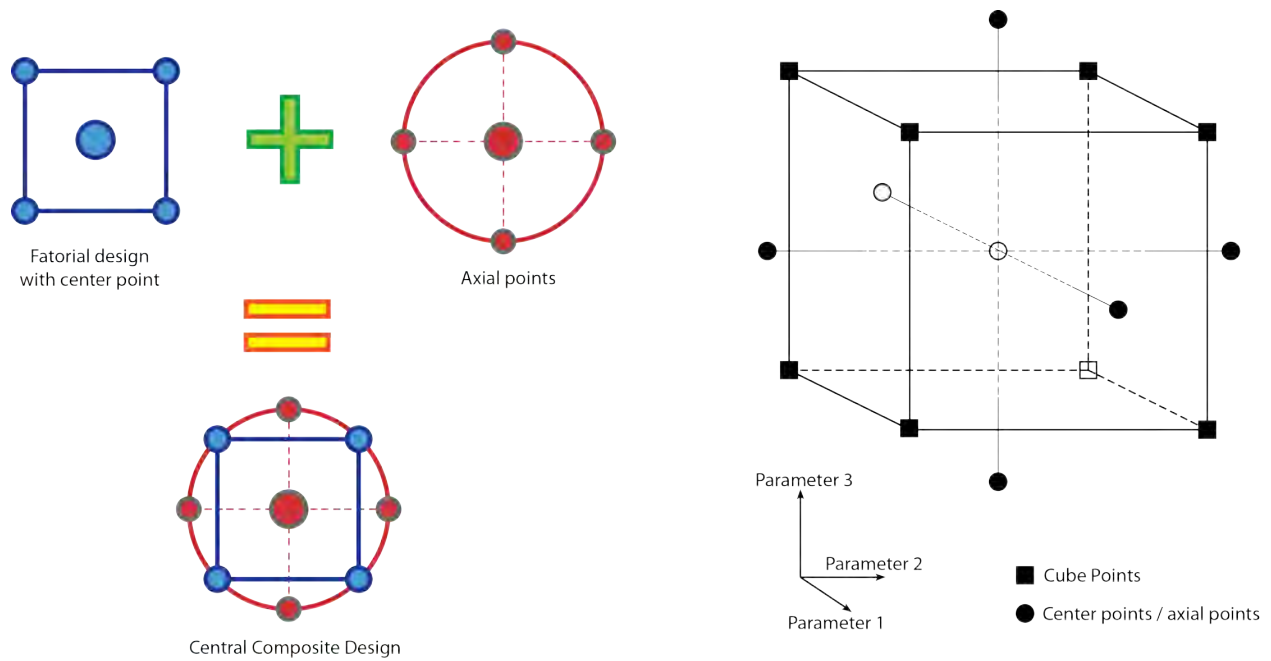


Figure 16 – Central composite design graphic representation

The total number of design points (n_e) depends on the number of factors and the number of center points (n_c). The total number of experimental trials is expressed in the equation below. The reasonable number of center points is typically three to five.

$$n_e = 2^k + 2k + n_c$$

Equation 7 – Eq. to calculate the number of design points

A central composite design consists of:

- A complete or fraction of a 2^k factorial design, where the factor levels are coded to the usual -1, +1 values. This is called the factorial portion of design.
- n_o center points ($n_o \geq 1$).
- Two axial points on the axis of each design variable at a distance of α from the design center. This portion is called the axial portion of the design.

The areas of flexibility in the use of the central composite design reside in the selection of α , the axial distance, and n_c , the number of center runs. The choice of α depends to a great extent on the region of operability and region of interest.

The choice of n_c often has an influence on the distribution of $N \text{Var} [\hat{y}(x)]/\sigma^2$ in the region of interest. [11] The result of the design involves F factorial points, $2k$ axial points and n_c center runs. Center runs clearly provide information about the existence of a curvature in the system. If curvature is found in the system, the addition points allow for efficient estimation of the pure quadratic terms. [9]

2.11 Box-Behnken Design

Box-Behnken designs are a class of rotatable or near rotatable second order designs based on three level incomplete factorial designs. For three factors its graphical representation can be perceived in two forms:

A cube that consists of the central point and the middle points of the edges, as can be observed in figure 17.

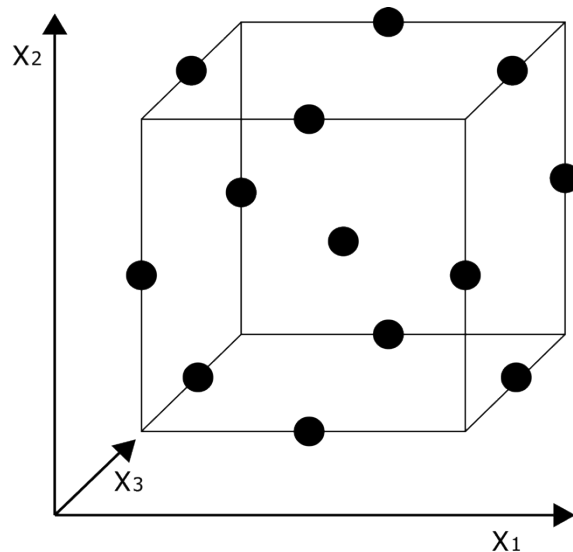


Figure 17 – The cube for BBD representation

A figure of three interlocking 2^2 factorial designs and a center point as observed in Fig. 18. The number of experiments (N) required for the development of BBD is defined as $N=2k(k-1)+C_0$, (where k is number of factors and C_0 is the number of center points). For comparison, the number of experiments for a central composite design is $N=2^k+2k+C_0$. An advantage of the BBD is that it does not contain combinations for which all factors are simultaneously at their highest or lowest levels. So these designs are practical for avoiding experiments performed under extreme conditions, for which unsatisfactory results might occur. Contrariwise, they are not designated for circumstances in which we would like identify the responses at the extremes, that is, at the vertices of the cube. [14] The BBD requires three levels of each factor instead of five as in the CCD, which result in fewer experimental trials to evaluate multiple variables and their interactions. [15]

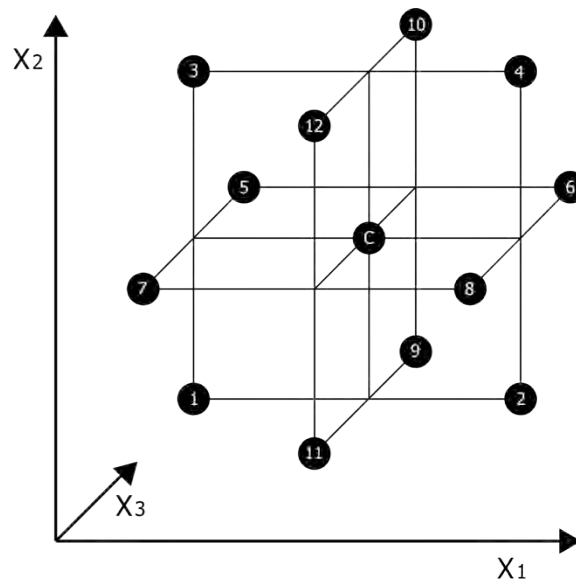


Figure 18 – 2^2 interlocking factorial design

CHAPTER 3

METHODOLOGY

The experiment consist on a real life experiment where the main objective is to collect enough data to be able to study, predict and/or observe the behavior of the assembled system. For this purpose the methodologies selected were CCD and Box-Behnken design, both are second order designs. One of the reasons to choose these methodologies is that a second order function was needed because it was important to observe if the behavior of the system had these characteristics.

The components used on the experiment were two different solar panels (one monocrystalline and one polycrystalline with the same characteristics, this ones taken as blocks, comparing their output power), the panels were also tested in 3 different environmental temperatures, one at the manufacturers recommendation (25° C), one at 65° C and the other one at -15° C (two more temperatures for the CCD are going to be used, 5° and 45° C, this because the methodology need 2 extra points for the axial point evaluation), also 3 different light angles were used(the angle on which the panel is receiving the light directly, the angles are defined on table 4). The angle was measured from the horizontal axis to the panel's axis just as it is illustrated on the next figure.

The last factor was the light color, for this factor it was decided to use only three levels (2500K, 5000K and 7000K). Three light sources (three light sources have been selected with similar amount of lumens but with three different colors). The system also used a very simple electronic circuit shown on fig. 21 (just to induce the flow of current and be able to measure not only the output voltage but also the current of the panel). Figure 20 shows a rough description on how the system looks like.

Panel angle and light incidence angle

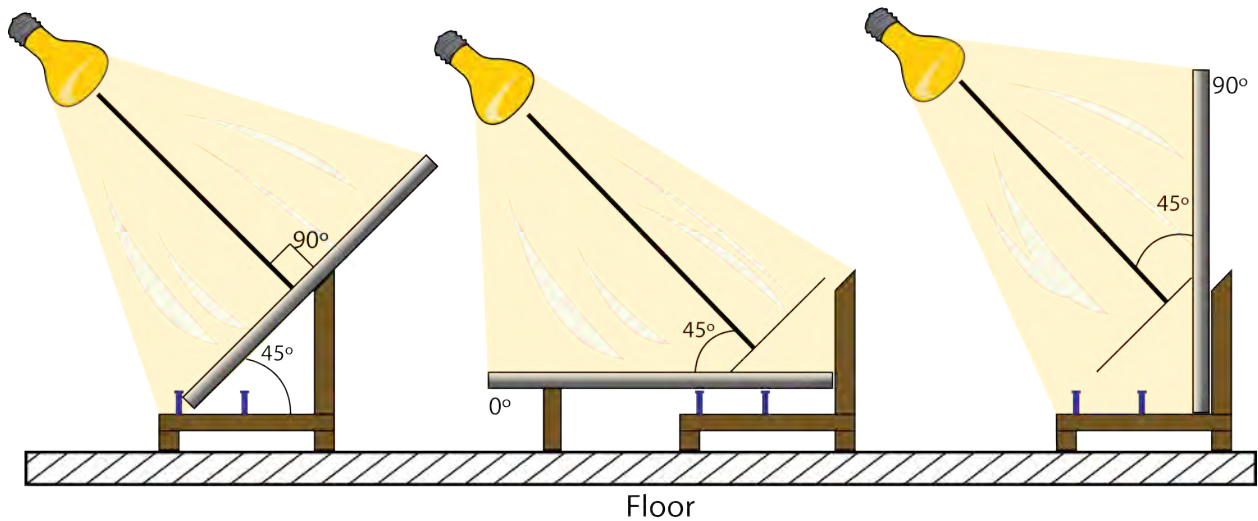


Figure 19 – Right view of the panel angle and light incidence angle

The intention with this is to create a successful experiment design being analyzed with central composite design and compared with a Box-Behnken design, in which the data recorded from each one of the experiments could be enough to come up with evidence and conclusions to be able to determine the optimum point of operation.

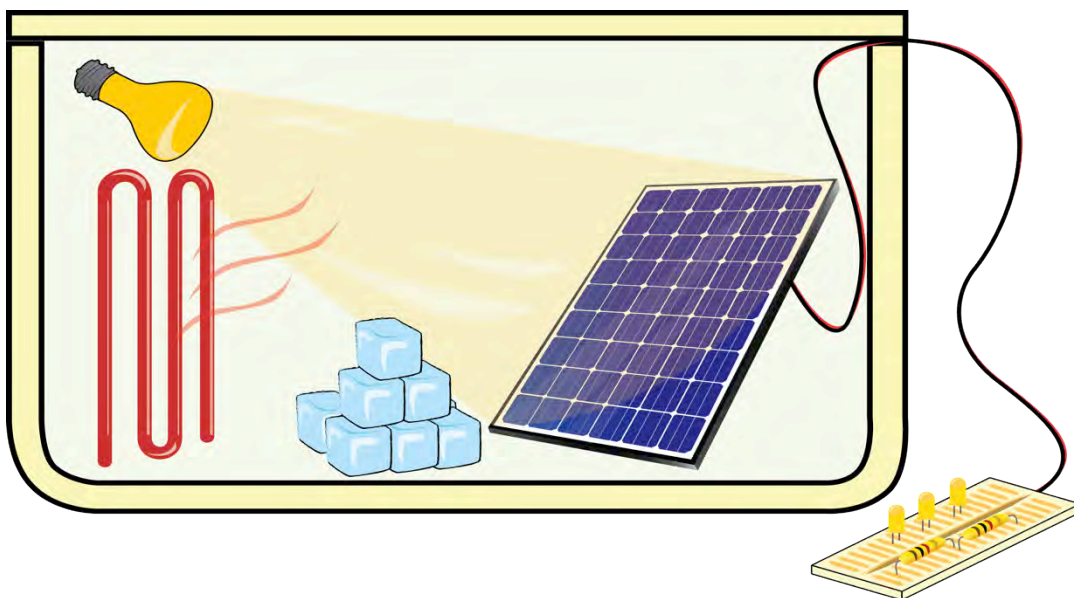


Figure 20 – Experiment schematic representation

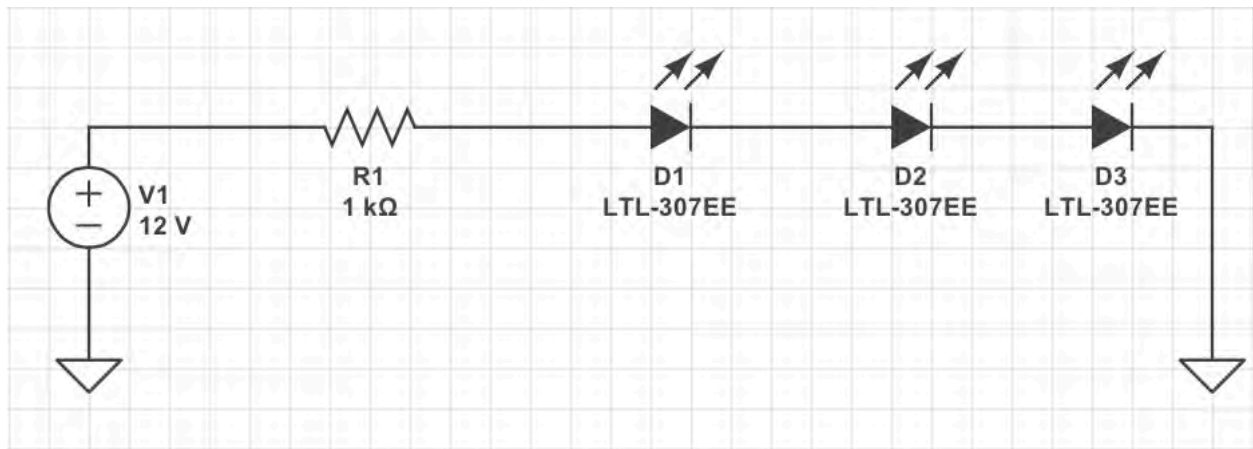


Figure 21 – Circuit diagram representation

The different factors are described in the following table.

Table 4 - Table of levels and factors for the experiment

Factors	Label (Levels)	Description
Temperature (A)	-2	-15 ° C
	-1	5° C (CCD only)
	0	25° C
	1	45° C (CCD only)
	2	65° C
Light Angle (B)	-2	90°
	-1	67.5° (CCD only)
	0	45°
	1	22.5° (CCD only)
	2	0°
Light Color (C)	-1	2500K
	0	5000K
	1	7500K

The experiment will need a controlled environment, so for the ambient temperature test a big box will be used to maintain the temperature for the different events of the experiment. (The use of a box it is not to maintain the temperature but to control that the amount of light that the panel is receiving is the same in all cases) The fridge will be used for the low temperature events and also a domestic oven for the hot temperature events. Throughout the experiment a precision digital thermometer will be used to verify that in all the

different events the conditions can be always the same for the different events and with this avoid variability and errors in the experiment.

At the time of the experiment, the record of the output power will be taken once all the components are on its place, making sure that the light bulb it is placed with the correct angle and the temperature reach the correct level. After this, there will be a repeated measurement process 5, so there will be 5 records for each run and each repeated measurement will be taken within five minute horizon time and ensuring that the temperature doesn't differ more than $\pm 5^{\circ}$ C from the original temperature. Also the experiment was designed taking in count two blocks defined because of the different kind of panels used on the experiment.

The next table (Table 5) shows both central composite and Box-Behnken design parameters specifically for this experiment.

Table 5 - Central composite and Box-Behnken design parameters

Central Composite Design		Box-Behnken Design	
Factors: 3	Replicates: 2	Factors: 3	Replicates: 2
Base runs: 20	Total runs: 40	Base runs: 15	Total runs: 60
Base blocks: 2	Total blocks: 2	Base blocks: 2	Total blocks: 2
Cube points: 16			
Center points: 8	α : 1.633	Center points: 6	
Axial points: 12			

Time to perform experiment:

Set-up for each run: 25 min. (105 total runs)

Record output:

CCD: 900 min. (25 min. X 40) BBD: 675 min. (25 min. X 60)

Total time: 5126 min. (85.4 hrs.)

The design matrix for CCD and Box-Behnken design are shown in the following tables.

Table 6 – CCD Design Matrix

StdOrder	RunOrder	Blocks	Temp	Angle	Light Color
32	1	1	25	45	4000
11	2	1	25	45	4000
31	3	1	25	45	4000
27	4	1	5	67.5	5000
9	5	1	25	45	4000
29	6	1	25	45	4000
21	7	1	5	22.5	3000
5	8	1	5	22.5	5000
25	9	1	5	22.5	5000
2	10	1	45	22.5	3000
30	11	1	25	45	4000
23	12	1	5	67.5	3000
3	13	1	5	67.5	3000
1	14	1	5	22.5	3000
22	15	1	45	22.5	3000
8	16	1	45	67.5	5000
28	17	1	45	67.5	5000
6	18	1	45	22.5	5000
12	19	1	25	45	4000
26	20	1	45	22.5	5000
4	21	1	45	67.5	3000
7	22	1	5	67.5	5000
24	23	1	45	67.5	3000
10	24	1	25	45	4000
37	25	2	25	45	300
20	26	2	25	45	4000
35	27	2	25	8.2575	4000
16	28	2	25	81.7425	4000
33	29	2	-7.66	45	4000
39	30	2	25	45	4000
38	31	2	25	45	500
19	32	2	25	45	4000
36	33	2	25	81.7425	4000
14	34	2	57.66	45	4000
13	35	2	-7.66	45	4000
17	36	2	25	45	3000
40	37	2	25	45	4000
18	38	2	25	45	500
15	39	2	25	8.2575	4000
34	40	2	57.66	45	4000

Table 7 – Box-Behnken design matrix

StdOrder	RunOrder	Blocks	Temp	Angle	Light Color
11	1	1	25	0	5000
29	2	1	25	45	4000
17	3	1	65	0	4000
8	4	1	65	45	5000
24	5	1	25	0	3000
15	6	1	25	45	4000
12	7	1	25	90	5000
4	8	1	65	90	4000
20	9	1	-15	45	3000
14	10	1	25	45	4000
6	11	1	65	45	3000
25	12	1	25	90	3000
28	13	1	25	45	4000
16	14	1	-15	0	4000
27	15	1	25	90	5000
13	16	1	25	45	4000
10	17	1	25	90	3000
18	18	1	-15	90	4000
19	19	1	65	90	4000
2	20	1	65	0	4000
5	21	1	-15	45	3000
30	22	1	25	45	4000
3	23	1	-15	90	4000
22	24	1	-15	45	5000
7	25	1	-15	45	5000
26	26	1	25	0	5000
23	27	1	65	45	5000
9	28	1	25	0	3000
1	29	1	-15	0	4000
21	30	1	65	45	3000
32	31	2	65	0	4000
41	32	2	25	0	5000
40	33	2	25	90	3000
36	34	2	65	45	3000
47	35	2	65	0	4000
37	36	2	-15	45	5000
49	37	2	65	90	4000
58	38	2	25	45	4000
43	39	2	25	45	4000
56	40	2	25	0	5000
51	41	2	65	45	3000
33	42	2	-15	90	4000
42	43	2	25	90	5000
52	44	2	-15	45	5000
31	45	2	-15	0	4000
50	46	2	-15	45	3000
54	47	2	25	0	3000
35	48	2	-15	45	3000
53	49	2	65	45	5000
39	50	2	25	0	3000
46	51	2	-15	0	4000
44	52	2	25	45	4000
34	53	2	65	90	4000
57	54	2	25	90	5000
45	55	2	25	45	4000
60	56	2	25	45	4000
59	57	2	25	45	4000
55	58	2	25	90	3000
38	59	2	65	45	5000
48	60	2	-15	90	4000

Table 8 – Table of tools and equipment used with descriptions

Tool/Equipment	Description
Multimeter	Craftsman 82139 Auto-ranging
Thermometer	Extech 401014 Indoor/Outdoor Thermometer. Range: -58 to 158-Degrees F (-50 to 70 Degrees C)
Fridge	Frigidaire - 18.2 Cu. Ft.
Oven	Hotpoint 5 cu. ft. Electric Range
Monocrystalline panel	Instapark 5.0 W SYP5S-M Max Power: 5.0 W Voc: 22.0 V Isc: 0.31 A Dimensions: 201*280*20
Polycrystalline panel	Instapark 5.0 W SYP5S-P Max Power: 5.0 W Voc: 22.0 V Isc: 0.31 A Dimensions: 201*280*20

CHAPTER 4

CASE OF STUDY

Before starting the experiment, the first thing done was to determine the time for the system to stabilize within the temperature of the environment whether it was cold or hot (3 trials were made before starting the experiment). The way of doing this was to put the system under testing conditions, the setup was the panel with a 45° angle, starting with a 25° temperature and lowering it until -15° and taking measurements every 5 seconds, this with the intention of observe how much time takes the panel to stabilize on the lower temperature of the experiment. After doing this test, the same was done but for high temperatures, starting at 25° and rising the temperature to 65°.

It was determined that a safe time for the setup of the system to stabilize before taking the measurements was between 15 and 20 minutes for cold temperatures and between 5 and 10 minutes for the hot temperatures. As for the ambient temperature, the system does not require this time because the panels and the whole system are already at the ambient temperature (The results are shown on the figure 22).

After knowing the setup time, the experiment occurs without any other complication, and following the methodologies described before, the data collection for both design matrixes took place. A timer was set to indicate the measurement of the temperature, voltage and current every 5 minutes and with these two numbers calculate the power, this whit the intention of collecting 5 repeated measurements, and at the end, have a better understanding of the system behavior and of course, better quality results for the analysis of the experiment.

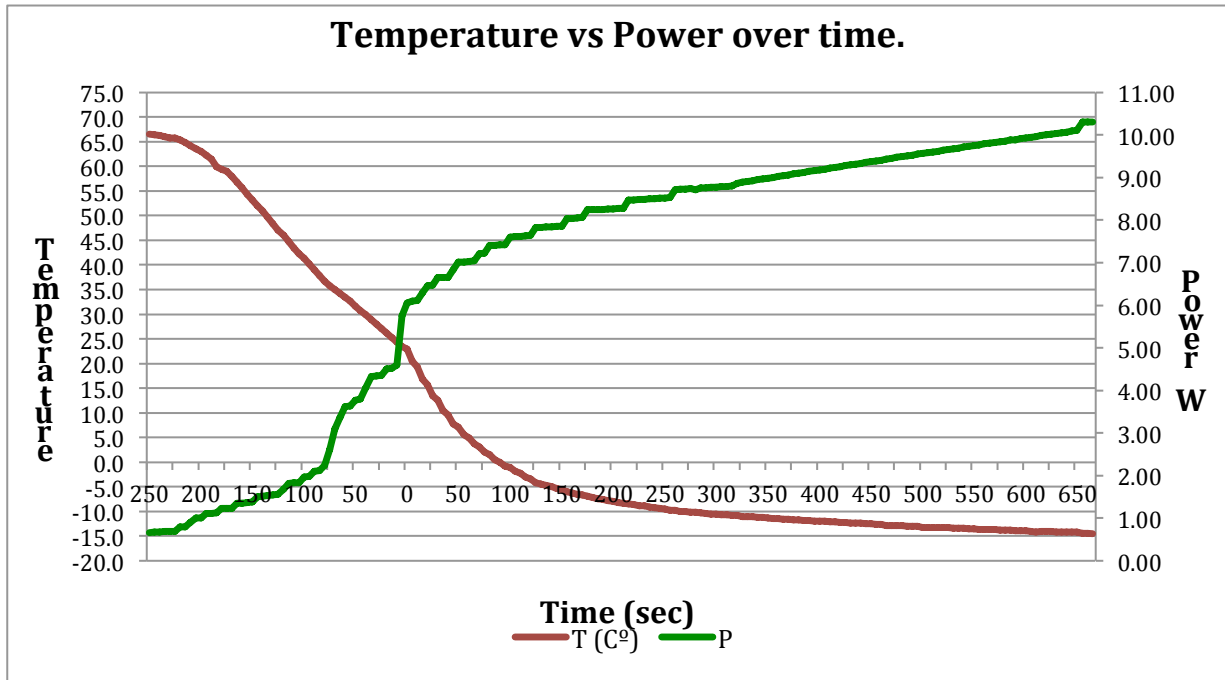


Figure 22 – Chart of Temperature vs. Power over time

The way of setting up every run of the experiment was first to check the parameters on the design matrix and set up the system inside the respective place, fridge for the cold runs, oven for the hot runs and the box for the 25° temperature runs. Then place the panel at the respective angle for that particular run and then setup the temperature on the oven or on the fridge, for the 25° temperatures it was not necessary to set up that parameter. After setting up the temperature it was necessary to wait the safe setup time of 15 to 20 min for the cold runs and 5 to 10 for the hot runs. Again, this was not necessary for the 25° temperature ones.

When the safe setup time was reached the first measurement was taken and the other 4 ones were taken with a 5 minutes interval between them. After the 5 measurements were taken, the process repeats until the whole experiment was finally finished. After the experiment was terminated, all the data was analyzed on the software Minitab. The software provides the significant factors that affect the system, which was our

objective. It also gives us useful chart like one for the normality testing, the response surface for the experiment and a contour plot.

Results

Table of results are shown first beginning with the CCD experiment. After, the results for the BBD are shown. CCD results table. *(For Complete results table see Annex A).*

Table 9 – Central Composite Design results table

StdOrder	Blocks	Temp	Angle	Light Color	Avg P (W)
1	1	5	22.5	3000	10.67
2	1	45	22.5	3000	4.23
3	1	5	67.5	3000	10.11
4	1	45	67.5	3000	4.39
5	1	5	22.5	5000	4.96
6	1	45	22.5	5000	1.41
7	1	5	67.5	5000	5.16
8	1	45	67.5	5000	2.12
9	1	25	45	4000	3.75
10	1	25	45	4000	4.08
11	1	25	45	4000	4.24
12	1	25	45	4000	4.76
13	2	-7.66	45	4000	11.00
14	2	57.66	45	4000	0.30
15	2	25	8.2575	4000	3.39
16	2	25	81.7425	4000	3.02
17	2	25	45	3000	1.84
18	2	25	45	5000	0.40
19	2	25	45	4000	2.64
20	2	25	45	4000	2.81
21	1	5	22.5	3000	11.25
22	1	45	22.5	3000	6.18
23	1	5	67.5	3000	11.08
24	1	45	67.5	3000	4.09
25	1	5	22.5	5000	5.44
26	1	45	22.5	5000	1.31
27	1	5	67.5	5000	5.14
28	1	45	67.5	5000	1.93
29	1	25	45	4000	3.62
30	1	25	45	4000	3.47
31	1	25	45	4000	4.66
32	1	25	45	4000	4.45
33	2	-7.66	45	4000	13.63
34	2	57.66	45	4000	0.67
35	2	25	8.2575	4000	2.33
36	2	25	81.7425	4000	2.19
37	2	25	45	3000	7.78
38	2	25	45	5000	0.53
39	2	25	45	4000	2.66
40	2	25	45	4000	2.47

BBD results table. (For Complete results table see Annex B).

Table 10 – Box-Behnken Design results table

StdOrder	Blocks	Temp	Angle	Light Color	Avg P (W)
1	1	-15	0	4000	11.53
2	1	65	0	4000	0.39
3	1	-15	90	4000	13.14
4	1	65	90	4000	0.87
5	1	-15	45	3000	13.33
6	1	65	45	3000	4.69
7	1	-15	45	5000	8.74
8	1	65	45	5000	0.32
9	1	25	0	3000	9.32
10	1	25	90	3000	8.84
11	1	25	0	5000	1.39
12	1	25	90	5000	2.36
13	1	25	45	4000	4.04
14	1	25	45	4000	2.20
15	1	25	45	4000	3.57
16	1	-15	0	4000	9.05
17	1	65	0	4000	0.55
18	1	-15	90	4000	10.83
19	1	65	90	4000	0.84
20	1	-15	45	3000	13.43
21	1	65	45	3000	4.51
22	1	-15	45	5000	8.76
23	1	65	45	5000	0.77
24	1	25	0	3000	8.99
25	1	25	90	3000	8.06
26	1	25	0	5000	1.41
27	1	25	90	5000	2.92
28	1	25	45	4000	4.09
29	1	25	45	4000	3.30
30	1	25	45	4000	3.56
31	2	-15	0	4000	5.50
32	2	65	0	4000	0.40
33	2	-15	90	4000	6.59
34	2	65	90	4000	0.53
35	2	-15	45	3000	8.80
36	2	65	45	3000	2.85
37	2	-15	45	5000	6.62
38	2	65	45	5000	0.19
39	2	25	0	3000	5.47
40	2	25	90	3000	6.19
41	2	25	0	5000	2.93
42	2	25	90	5000	1.43
43	2	25	45	4000	2.46
44	2	25	45	4000	2.01
45	2	25	45	4000	1.34
46	2	-15	0	4000	7.01
47	2	65	0	4000	0.45
48	2	-15	90	4000	7.99
49	2	65	90	4000	0.51
50	2	-15	45	3000	9.04
51	2	65	45	3000	2.75
52	2	-15	45	5000	5.32
53	2	65	45	5000	0.47
54	2	25	0	3000	5.67
55	2	25	90	3000	5.38
56	2	25	0	5000	0.86
57	2	25	90	5000	1.78
58	2	25	45	4000	2.17
59	2	25	45	4000	2.49
60	2	25	45	4000	2.16

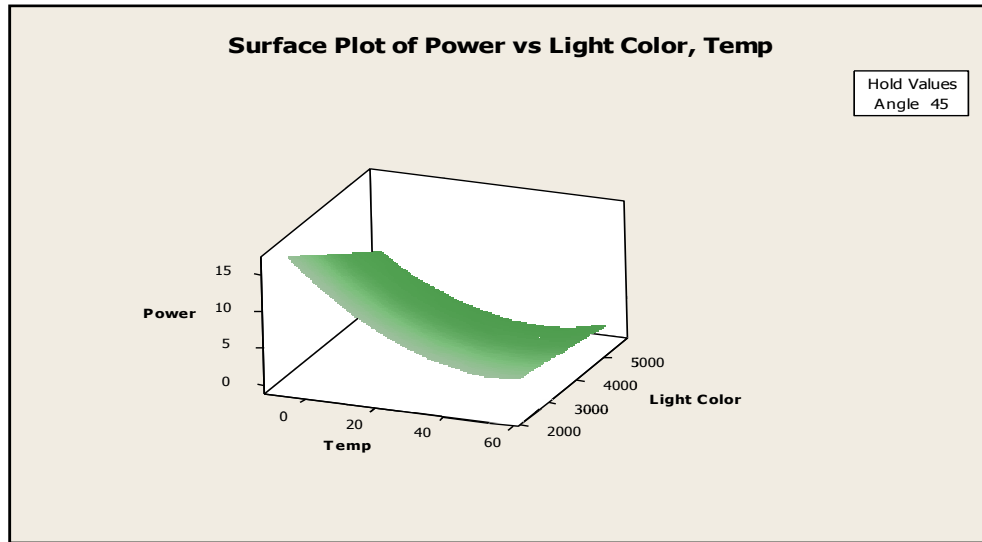


Figure 23 – CCD response surface plot

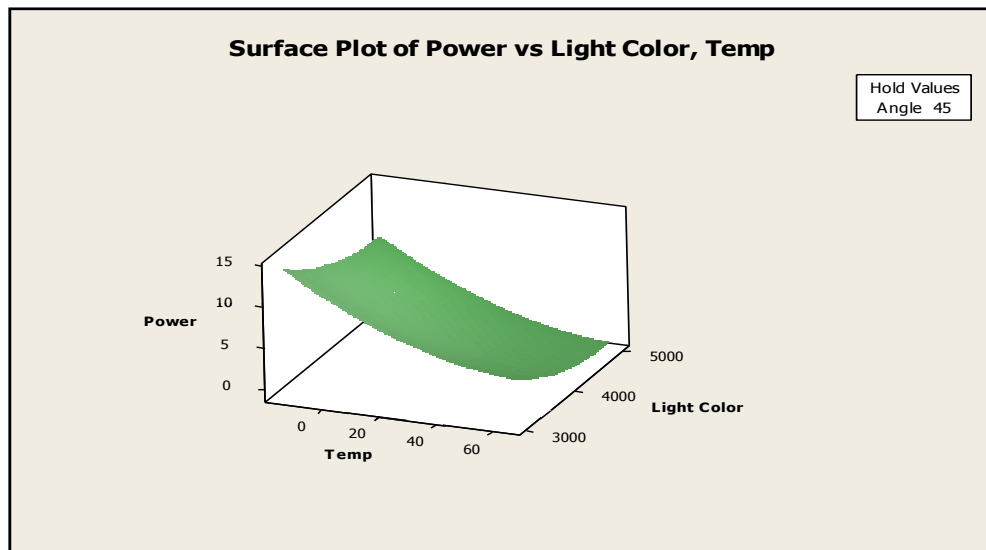


Figure 24 –BBD response surface plot

For both the CCD and BBD the results were very close and show a lot of consistency, and from both we can make the same conclusions.

The temperature, light color and panel type are very significant factors, while the angle is not significant for this experiment. Results are shown in table 10 for CCD and in table 11 for BBD.

Table 11 - Regression Coefficients for Power from CCD

Estimated Regression Coefficients for Power CCD analysis

Term	Coef SE	Coef	T	P
Constant	3.3824	0.344	9.822	0.000
Block	0.7504	0.1921	3.907	0.001
Temp	-2.8782	0.2305	-12.489	0.000
Angle	-0.0848	0.2305	-0.368	0.715
Light Color	-1.8268	0.2305	-7.927	0.000
Temp*Temp	1.4142	0.2316	6.107	0.000
Angle*Angle	0.0384	0.2316	0.166	0.869
Light color* Light Color	0.0032	0.2316	0.014	0.989
Temp*Angle	0.0152	0.2975	0.051	0.960
Temp*Light Color	0.6422	0.2975	2.159	0.039
Angle*Light Color	0.2419	0.2975	0.813	0.423

Table 12 - Regression Coefficients for Power from BBD

Estimated Regression Coefficients for Power BBD analysis

Term	Coef SE	Coef	T	P
Constant	3.4583	0.4005	8.636	0.000
Block	0.7504	0.1921	3.907	0.000
Temp	-4.7409	0.2452	-19.332	0.000
Angle	0.3276	0.2452	1.336	0.197
Light Color	-2.7808	0.2452	-11.339	0.000
Temp*Temp	1.9238	0.3610	5.329	0.000
Angle*Angle	0.5163	0.3610	1.430	0.168
Light color* Light Color	1.4358	0.3610	3.978	0.001
Temp*Angle	-0.3258	0.3468	-0.939	0.359
Temp*Light Color	0.1435	0.3468	0.414	0.683
Angle*Light Color	0.4864	0.3468	1.402	0.176

The significant factors are only the ones that have a P value under 0.05 and in both tables we have the same result with one exception. The same results are that the Block, Temp and Light Color are significant. The change is that for the CCD the other significant factor is the temperature square and Temperature times Light Color while on the BBD it is the Light Color square.

This is not a big change because the factors by itself were already significant without being square or intersected by another factor but the intersection means that the effect of one factor changes the value of the other factor and vice versa. The next expressions show the regression equations given by the CCD and BBD computational analysis.

$$y = 22.05 + 0.75B - 0.45T - 0.0031L + 0.0035T^2 + 3.21 \times 10^{-5}TL$$

Equation 8 – Regression analysis equation from CCD

$$y = 43.55 - 0.1848T - 0.0148L + 0.0012T^2 + 1.4358 \times 10^{-6}L^2$$

Equation 9 – Regression analysis equation from BBD

The results are also showing that the best conditions for a solar panel to work on its more efficient way are the following. Temperature -15°, Light Color 3000K and any angle, but it is recommended the direct hit of the light rays. (This conclusion is taken because the angle was not significant on the experiment). Also the experiment is showing that the monocrystalline panel is around 30% more efficient than the polycrystalline one (The comparison between the monocrystalline and the polycrystalline panel is shown in Fig 26), that's why the experiment is showing that the blocking is significant for the experiment (The two kinds of panels were taken as blocks for the experiment).

A confirmatory run was made to ensure that the results of the experiment were accurate. The results show and confirm that these factors produce the most power out of the panel. The results are shown on the next table.

Table 13 – Table of results for the 3 confirmatory runs

Temp	Angle	Light Color	P 1	P 2	P 3	P 4	P 5	Avrg. P (W)
-15	45	3000	13.34	13.59	13.91	13.96	14.03	13.76
-15	45	3000	12.80	13.21	13.57	13.96	14.00	13.51
-15	45	3000	12.99	13.67	14.43	14.25	14.43	13.95

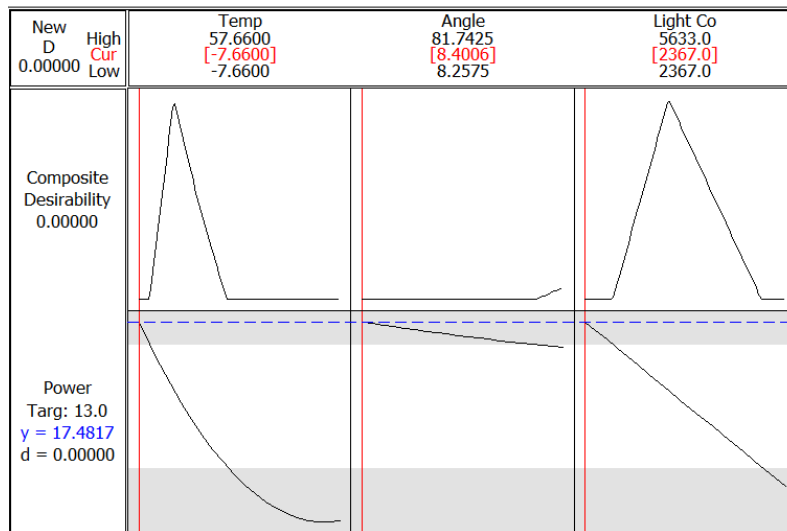


Figure 25 – Response surface optimization plot

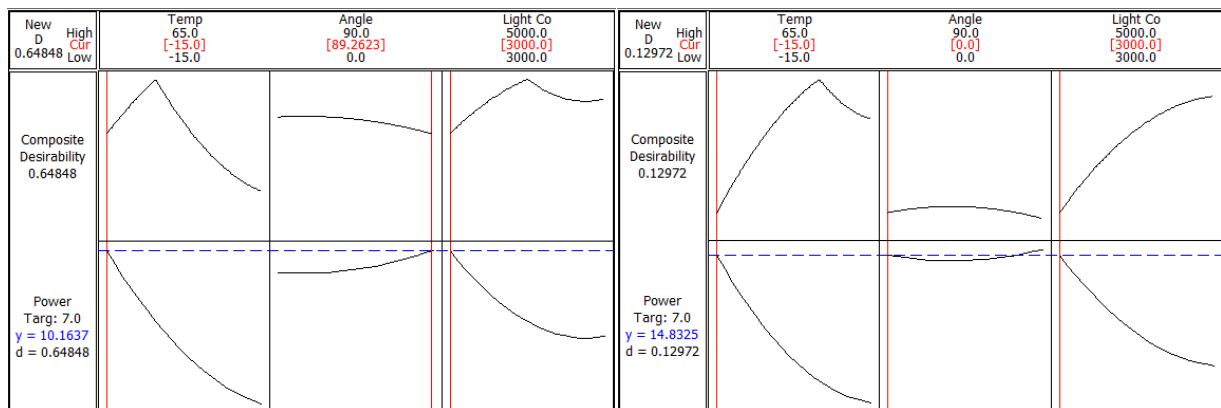


Figure 26 – Chart showing the optimal output from the polycrystalline panel (on the left) and the monocrystalline panel (on the right)

CHAPTER 5

DISCUSSIONS AND CONCLUSIONS

One of the problems faced during the experiment was that the equipment used for taking the measurements does not measure power, only voltage and current, so it was necessary to calculate it by using ohms law. Another one was the fact that the experiment could not be done inside a proper research lab and instead of this it was done on a particular house, with regular home appliances as equipment, this cause that the time to perform the experiment increase. For example, when the event occurs on a hot temperature it was needed to set up the temperature of the oven and during the whole event check the thermometer for any mayor change on the temperature, while at the same time taking the measurement and record them on the computer.

The output power efficiency of solar panels is directly correlated with the temperature, that's something that can be found in some articles and papers but as the experiment shows it is finally clear how much the temperature affects the output power efficiency on a solar panel. One of the most interesting things about this experiment was to discover that the color temperature of the light was one of the most important factors on the experiment and the fact that the color temperature of the sun light it is not the most effective one for the solar panels to convert light into electricity. The interesting part is that it is very hard to find a study that tells us how the solar panels behave with different color temperatures of light. Kreutzmann, A. (2006) says that the silicon transmit 95% of the wavelength of the infrared radiation, this can be one of the reasons why the panel behave better with a color light temperature near the infrared spectrum than with the color temperatures near the ultraviolet spectrum.

Another conclusion and a very important one is that the angle was not significant. Watching this give us a chance to think why a lot of efforts are centered on tracking systems and some other solutions to have the best angle of incidence instead of focusing all the resources on the color temperature of the light or on the temperature of the panel that are the most significant factors for a solar panel to produce electricity. Of course the angle plays an important factor on the electricity production, but it's on the third place.

A very important thing to conclude is the fact that the objectives were fulfilled with this work, leaving accurate and useful information regarding the studied system, and giving a new way on which these kinds of devices can be improved in the future. One more thing to make clear is that the contributions made by this experiment were new; the statement tries to say that it is not easy or there is not another experiment that tries to play with the factors like on this experiment.

Now, this experiment leads the way to a lot of new ideas like indoor solar cells instead of regular tile floor for all day and night production and maybe some other applications. As a future work, another experiment can be made to try to mimic a lower color temperature of the light with a kind of filter or tint on top of the solar panel to try to improve the efficiency of it. Also it would be very interesting to find the break point of the solar panel, break point meaning the point in which on hot temperatures the panel stop working completely and on cold temperatures try to observe if at any given temperature the panel start declining on its efficiency instead of increasing it, with the intention of look up for a solution to cool down the panels. This kind of study can be made only with a very precise controlled environment and high precision tools.

REFERENCES

- 1** - Paul Kruger. The quest for sustainable energy. Stanford University, Ed. John Wiley & Sons, 2006.
- 2** - British Petroleum. Energy – Consumption!A1 "Consumption by fuel, 1965–2008" (XLS). Statistical Review of World Energy 2009, 31 July 2006. Retrieved 24 October 2009.
- 3** - Aldo V. Da Rosa. Fundamentals of renewable energy processes, Stanford University, Elsevier academic press, 2005.
- 4** - Worldwatch Institute. State of the World 2009. 2009.
- 5** - S. Ranjan, S. Balaji, Rocco A. Panella, B. Erik Ydstie. Silicon solar cell production. Carnegie Mellon University, Department of Chemical Engineering, 5000 Forbes Avenue, Pittsburgh, PA 15213, United States; 2011.
- 6** - Jenny Nelson. The Physics of Solar Cells. Imperial College Press; 1 edition (September 5, 2003); 384 pages.
- 7** - US Department of Energy. "<http://energy.gov/science-innovation/energysources/renewable-energy/solar>".
- 8** - Douglas C. Montgomery. Design and Analysis of Experiments. Ed. John Wiley & Sons 7th Edition, 2009; 656 pages.
- 9** - Raymond H. Myers, Douglas C. Montgomery. Response Surface Methodology. Ed. John Wiley & Sons, 2002, 2d Edition.
- 10** - André I. Khuri, John A. Cornell. Response Surfaces Design and Analyses. Ed. Marcel Dekker, Inc. 1987.
- 11** - George C. Canavos, Ioannis A. Koutouvelis. An Introduction to the design & Analysis of Experiments. Ed Pearson Prentice Hall, 2009.
- 12** - NIST/SEMATECH, *e-Handbook of Statistical Methods*. <http://www.itl.nist.gov/div898/handbook/>, 2013.
- 13** - André I. Khuri, John A. Cornell. Response Surfaces: Designs and Analyses. Ed CRC Press, 1996, 510 pages.
- 14** - Thomas P. Ryan. Statistical Methods for Quality Improvement. Ed. John Wiley & Sons, 2011; 3d Edition
- 15** - Long Wu, Kit-lun Yick, Sun-pui Ng, Joanne Yip. Application of the Box–Behnken design to the optimization of process parameters in foam cup molding, Expert Systems with Applications, Volume 39, Issue 9, July 2012, Pages 8059–8065.
- 16** - N. Aslan. Application of response surface methodology and central composite rotatable design for modeling the influence of some operating variables of a Multi-Gravity Separator for coal cleaning. *Fuel*, Volume 86, Issues 5–6, March–April 2007, Pages 769–776.
- 17** - S.L.C. Ferreira, R.E. Bruns, H.S. Ferreira, G.D. Matos, J.M. David, G.C. Brandão, E.G.P. da Silva. Box-Behnken design: An alternative for the optimization of analytical methods. *Analytica Chimica Acta*, Volume 597, Issue 2, 10 August 2007, Pages 179–186, L.A. Portugal, P.S. dos Reis, A.S. Souza, W.N.L. dos Santos.

- 18-** Xiaojiao Wang, Gaihe Yang, Fang Li, Yongzhong Feng, Guangxin Ren, Xinhui Han. Evaluation of two statistical methods for optimizing the feeding composition in anaerobic co-digestion: Mixture design and central composite design. *Bioresource Technology*, Volume 131, March 2013, Pages 172-178.
- 19-** P. Angelopoulos, H. Evangelaras, C. Koukouvinos. Small, balanced, efficient and near rotatable central composite designs. *Journal of Statistical Planning and Inference*, Volume 139, Issue 6, 1 June 2009, Pages 2010-2013 P. Angelopoulos, H. Evangelaras, C. Koukouvinos.
- 20-** Yin Hang, Ming Qu, Satish Ukkusuri. Optimizing the design of a solar cooling system using central composite design techniques. *Energy and Buildings*, Volume 43, Issue 4, April 2011, Pages 988-994.
- 21-** Sabir Rustemli, Furkan Dincer, Emin Unal, Muharrem Karaaslan, Cumali Sabah. The analysis on sun tracking and cooling systems for photovoltaic panels. *Renewable and Sustainable Energy Reviews*, Volume 22, June 2013, Pages 598–603.
- 22-** Rosenberger James. Box-Behnken Designs. Published on STAT 503 - Design of Experiments course, Pennstate University.
- 23-** David J. Edwards. Fractional Box-Behnken Designs. Department of Statistical Sciences and Operations Research, Virginia Commonwealth University Richmond, VA.
- 24-** E. Skoplaki, J.A. Palyvos. On the temperature dependence of photovoltaic module electrical performance: A review of efficiency/power correlations. *Solar Energy*, Volume 83, Issue 5, May 2009, Pages 614–624.
- 25-** Xiaojiao Wang, Gaihe Yang, Fang Li, Yongzhong Feng, Guangxin Ren, Xinhui Han. Evaluation of two statistical methods for optimizing the feeding composition in anaerobic co-digestion: Mixture design and central composite design. *Bioresource Technology*, Volume 131, March 2013, Pages 172–178.
- 26-** M. Usama Siddiqui, A.F.M. Arif, Leah Kelley, Steven Dubowsky. Three-dimensional thermal modeling of a photovoltaic module under varying conditions. *Solar Energy*, Volume 86, Issue 9, September 2012, Pages 2620–2631.
- 27-** E.D. Mehleri, P.L. Zervas, H. Sarimveis, J.A. Palyvos, N.C. Markatos. Determination of the optimal tilt angle and orientation for solar photovoltaic arrays. *Renewable Energy*, Volume 35, Issue 11, November 2010, Pages 2468–2475
- 28-** H.M.S. Hussein, G.E. Ahmad, H.H. El-Ghetany. Performance evaluation of photovoltaic modules at different tilt angles and orientations. *Energy Conversion and Management*, Volume 45, Issues 15–16, September 2004, Pages 2441–2452.
- 29-** G.M. Tina, M. Rosa-Clot, P. Rosa-Clot, P.F. Scandura. Optical and thermal behavior of submerged photovoltaic solar panel: SP2. *Energy*, Volume 39, Issue 1, March 2012, Pages 17–26.

APPENDIX A

CCD complete Results

Repeated measurements																										Avrg P (W)
StdOr der	RunO rder	Blo ck	Temp	Angle	Light Color	T 1	V 1	C 1	P 1	T 2	V 2	C 2	P 2	T 3	V 3	C 3	P 3	T 4	V 4	C 4	P 4	T 5	V 5	C 5	P 5	
32	1	1	25	45	4000	24.6	15.96	0.30	4.79	25.2	15.50	0.29	4.50	25.3	15.42	0.29	4.47	25.6	15.22	0.28	4.26	25.8	15.13	0.28	4.24	4.45
11	2	1	25	45	4000	24.8	15.74	0.25	3.94	25.2	15.44	0.29	4.48	25.4	15.30	0.28	4.28	25.6	15.22	0.28	4.26	25.7	15.17	0.28	4.25	4.24
31	3	1	25	45	4000	24.7	15.95	0.31	4.94	24.9	15.71	0.30	4.71	25.1	15.58	0.30	4.67	25.4	15.48	0.29	4.49	25.6	15.40	0.29	4.47	4.66
27	4	1	5	67.5	5000	5.8	14.90	0.33	4.92	5.4	15.04	0.34	5.11	5.3	15.13	0.34	5.14	5.00	15.21	0.34	5.17	4.80	15.27	0.35	5.34	5.14
9	5	1	25	45	4000	24.3	15.16	0.28	4.24	24.6	14.82	0.28	4.15	24.9	14.69	0.24	3.53	24.9	14.57	0.23	3.35	25.1	14.52	0.24	3.48	3.75
29	6	1	25	45	4000	24.6	14.88	0.26	3.87	24.6	14.62	0.25	3.66	24.9	14.54	0.25	3.64	25.0	14.50	0.24	3.48	25.1	14.45	0.24	3.47	3.62
21	7	1	5	22.5	3000	6.3	20.11	0.57	11.46	5.6	20.03	0.56	11.22	5.5	20.00	0.56	11.20	5.6	19.96	0.56	11.18	5.7	19.95	0.56	11.17	11.25
5	8	1	5	22.5	5000	5.4	14.63	0.32	4.68	4.0	14.89	0.33	4.91	5.4	14.93	0.33	4.92	3.7	15.07	0.34	5.12	3.0	15.16	0.34	5.15	4.96
25	9	1	5	22.5	5000	3.4	15.25	0.33	5.03	3.3	15.35	0.35	5.37	1.9	15.50	0.36	5.58	1.3	15.58	0.36	5.60	1.2	15.59	0.36	5.61	5.44
2	10	1	45	22.5	3000	46.5	15.41	0.34	5.24	47.5	13.86	0.29	4.02	48.5	13.65	0.27	3.68	47.0	13.95	0.29	4.04	44.5	14.28	0.29	4.14	4.23
30	11	1	25	45	4000	24.4	14.54	0.25	3.64	26.4	14.64	0.25	3.66	26.7	14.56	0.25	3.64	26.6	14.54	0.20	2.908	26.5	14.58	0.24	3.50	3.47
23	12	1	5	67.5	3000	6.1	19.77	0.54	10.68	4.2	19.88	0.56	11.13	4.0	19.97	0.56	11.18	4.0	19.98	0.56	11.18	4.1	19.99	0.56	11.19	11.08
3	13	1	5	67.5	3000	6.0	18.91	0.51	9.64	4.1	19.18	0.49	9.40	3.5	19.59	0.53	10.38	3.2	19.51	0.54	10.53	3.1	19.59	0.54	10.57	10.11
1	14	1	5	22.5	3000	6.8	19.71	0.52	10.25	5.2	19.66	0.55	10.81	4.6	19.67	0.55	10.81	4.2	19.68	0.54	10.62	4.1	19.70	0.55	10.83	10.67
22	15	1	45	22.5	3000	44.8	16.73	0.41	6.86	45.3	16.36	0.39	6.38	44.4	16.24	0.34	5.52	48.2	15.99	0.38	6.07	47.0	15.98	0.38	6.07	6.18
8	16	1	45	67.5	5000	48.2	11.21	0.17	1.91	47.5	11.18	0.16	1.79	44.6	11.42	0.18	2.05	43.6	15.53	0.18	2.80	44.2	11.44	0.18	2.05	2.12
28	17	1	45	67.5	5000	47.2	11.23	0.17	1.91	48.5	11.18	0.16	1.79	46.5	11.25	0.17	1.91	44.5	11.42	0.17	1.94	43.0	11.57	0.18	2.08	1.93
6	18	1	45	22.5	5000	43.4	10.49	0.13	1.36	48.0	10.13	0.12	1.22	42.8	10.55	0.13	1.37	43.6	10.57	0.14	1.47	40.0	10.94	0.15	1.64	1.41
12	19	1	25	45	4000	24.5	16.21	0.32	5.19	26.0	15.91	0.31	4.93	26.9	15.67	0.30	4.70	27.5	15.53	0.29	4.50	27.8	15.39	0.29	4.46	4.76
26	20	1	45	22.5	5000	44.2	10.54	0.13	1.37	47.2	10.20	0.12	1.22	43.2	10.36	0.13	1.34	43.9	10.31	0.12	1.23	42.0	10.47	0.13	1.36	1.31
4	21	1	45	67.5	3000	49.5	14.03	0.29	4.07	46.6	14.23	0.30	4.27	45.0	14.35	0.31	4.44	43.7	14.49	0.31	4.49	42.1	14.65	0.32	4.68	4.39
7	22	1	5	67.5	5000	7.5	14.69	0.32	4.70	6.2	14.98	0.33	4.94	5.9	15.27	0.35	5.34	5.6	15.38	0.35	5.38	5.3	15.45	0.35	5.40	5.16
24	23	1	45	67.5	3000	45.5	13.89	0.29	4.03	43.5	13.88	0.28	3.89	42.5	13.96	0.29	4.04	42.1	14.63	0.33	4.82	41.8	13.63	0.27	3.68	4.09
10	24	1	25	45	4000	24.1	15.65	0.30	4.70	24.1	15.16	0.28	4.24	24.2	15.02	0.26	3.90	25.0	14.89	0.26	3.87	25.5	14.70	0.25	3.67	4.08
37	25	2	25	45	2367	25.0	17.03	0.43	7.32	24.1	17.02	0.42	7.15	26.5	17.66	0.46	8.12	25.5	17.73	0.46	8.15	26.8	17.67	0.46	8.12	7.78
20	26	2	25	45	4000	23.5	14.18	0.23	3.26	24.4	13.87	0.22	3.05	24.9	13.70	0.20	2.74	25.1	13.45	0.20	2.69	25.1	13.43	0.17	2.28	2.81
35	27	2	25	8.25	4000	25.4	13.00	0.18	2.34	25.5	12.98	0.18	2.34	25.0	12.97	0.18	2.33	25.5	12.92	0.18	2.32	25.8	12.86	0.18	2.31	2.33
16	28	2	25	81.74	4000	24.8	12.17	0.25	3.04	24.9	13.09	0.24	3.14	25.0	13.01	0.23	2.99	25.2	12.92	0.23	2.97	25.8	12.85	0.23	2.95	3.02
33	29	2	-7.66	45	4000	-18.9	21.59	0.56	12.09	-19.8	22.36	0.60	13.42	-21.5	22.84	0.62	14.16	-21.8	22.92	0.62	14.21	-22.1	22.99	0.62	14.25	13.63
39	30	2	25	45	4000	25.7	13.87	0.22	3.05	25.5	13.49	0.20	2.70	25.3	13.34	0.19	2.53	25.2	13.30	0.19	2.52	25.1	13.18	0.19	2.50	2.66
38	31	2	25	45	5633	24.9	8.41	0.07	0.59	24.5	8.36	0.07	0.59	24.9	8.38	0.06	0.50	24.4	8.19	0.06	0.49	24.1	8.17	0.06	0.49	0.53
19	32	2	25	45	4000	24.3	13.60	0.22	2.99	24.7	13.64	0.20	2.73	25.1	13.36	0.18	2.40	25.0	13.34	0.19	2.53	24.9	13.24	0.19	2.51	2.64
36	33	2	25	81.74	4000	25.0	13.04	0.17	2.22	25.5	12.88	0.17	2.19	25.5	12.85	0.17	2.18	25.3	12.78	0.17	2.17	25.3	12.79	0.17	2.17	2.19
14	34	2	57.66	45	4000	56.6	9.62	0.04	0.38	61.2	9.54	0.04	0.38	64.7	9.17	0.03	0.27	61.2	9.1	0.02	0.18	58.5	9.35	0.03	0.28	0.30
13	35	2	-7.66	45	4000	-8.8	20.04	0.48	9.62	-13.3	20.34	0.50	10.17	-16.5	21.15	0.54	11.42	-18.7	21.37	0.55	11.75	-19.7	21.50	0.56	12.04	11.00
17	36	2	25	45	2367	25.1	11.37	0.16	1.82	24.8	11.31	0.17	1.92	25.1	11.23	0.17	1.90	25.5	11.16	0.16	1.78	25.8	11.13	0.16	1.78	1.84
40	37	2	25	45	4000	25.3	13.31	0.19	2.53	26.0	13.24	0.18	2.38	26.3	13.25	0.19	2.51	26.2	13.25	0.19	2.51	26.2	13.25	0.18	2.38	2.47
18	38	2	25	45	5633	25.0	7.98	0.04	0.32	24.6	7.92	0.05	0.40	24.5	7.92	0.05	0.40	24.6	7.98	0.05	0.40	24.6	8.02	0.06	0.48	0.40
15	39	2	25	8.25	4000	24.3	14.93	0.26	3.88	24.9	14.60	0.23	3.36	25.0	14.33	0.22	3.15	25.0	14.27	0.23	3.28	25.5	14.15	0.23	3.25	3.39
34	40	2	57.66	45	4000	59.8	11.68	0.12	1.40	61.1	10.0	0.05	0.50	59.8	11.74	0.04	0.46	56.6	9.84	0.05	0.492	55.2	9.91	0.05	0.49	0.67

Central Composite Design

Factors: 3 Replicates: 2
Base runs: 20 Total runs: 40
Base blocks: 2 Total blocks: 2

Two-level factorial: Full factorial

Cube points: 16
Center points in cube: 8
Axial points: 12
Center points in axial: 4

Alpha: 1.633

Response Surface Regression: Power versus Block, Temp, Angle, Light Color

The analysis was done using coded units.

Estimated Regression Coefficients for Power

Term	Coef	SE Coef	T	P
Constant	3.38243	0.3444	9.822	0.000
Block	0.75041	0.1921	3.907	0.001
Temp	-2.87828	0.2305	-12.489	0.000
Angle	-0.08488	0.2305	-0.368	0.715
Light Color	-1.82689	0.2305	-7.927	0.000
Temp*Temp	1.41426	0.2316	6.107	0.000
Angle*Angle	0.03845	0.2316	0.166	0.869
Light Color*Light Color	0.00328	0.2316	0.014	0.989
Temp*Angle	0.01524	0.2975	0.051	0.960
Temp*Light Color	0.64227	0.2975	2.159	0.039
Angle*Light Color	0.24192	0.2975	0.813	0.423

S = 1.19011 PRESS = 92.6007

R-Sq = 90.53% R-Sq(pred) = 78.64% R-Sq(adj) = 87.26%

Analysis of Variance for Power

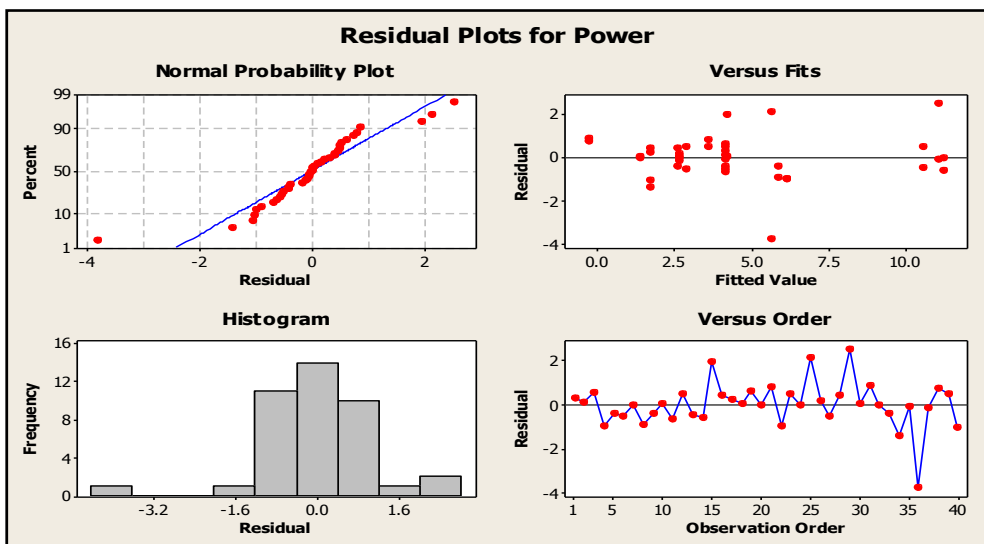
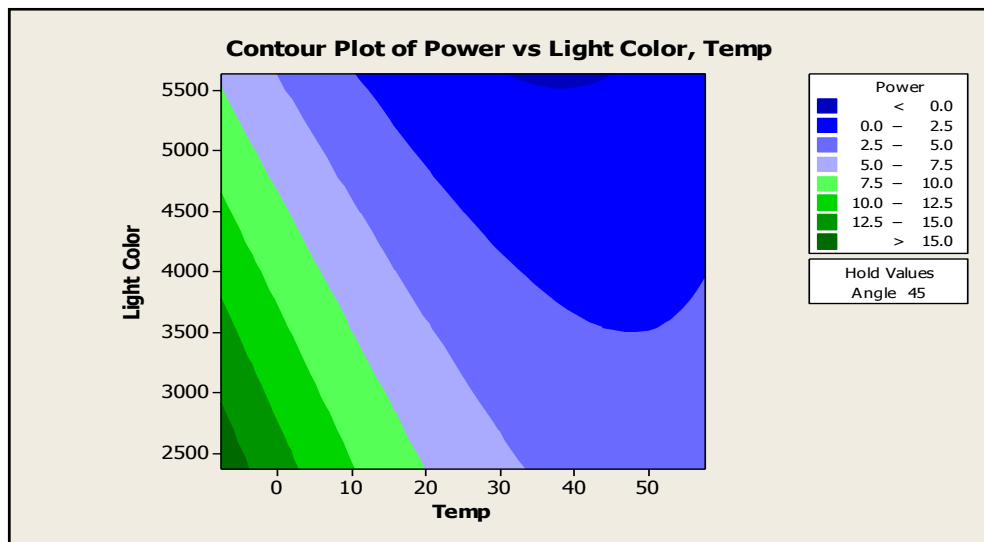
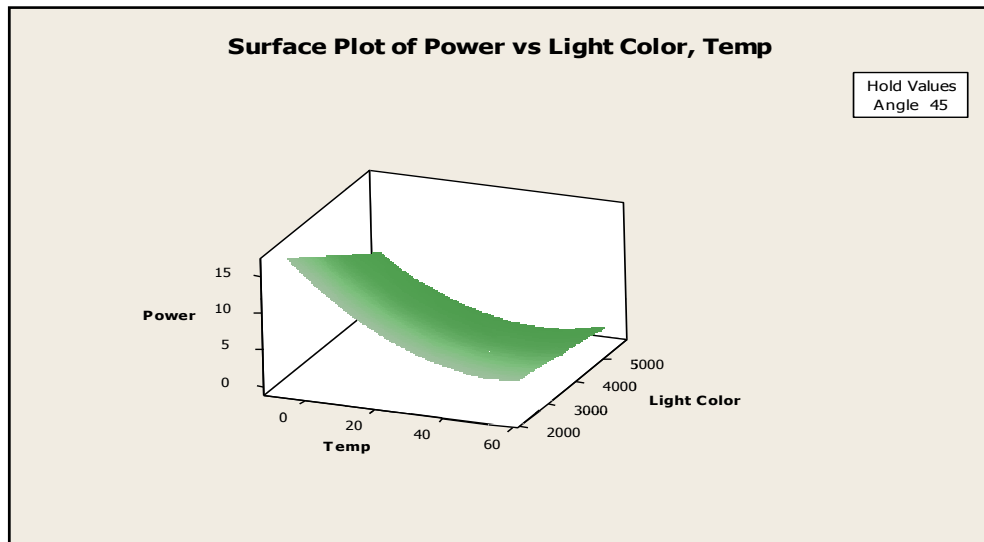
Source	DF	Seq SS	Adj SS	Adj MS	F	P
Blocks	1	21.623	21.624	21.624	15.27	0.001
Regression	9	370.820	370.820	41.202	29.09	0.000
Linear	3	310.113	310.113	103.371	72.98	0.000
Temp	1	220.920	220.920	220.920	155.98	0.000
Angle	1	0.192	0.192	0.192	0.14	0.715
Light Color	1	89.001	89.001	89.001	62.84	0.000
Square	3	53.167	53.167	17.722	12.51	0.000
Temp*Temp	1	53.128	52.829	52.829	37.30	0.000
Angle*Angle	1	0.039	0.039	0.039	0.03	0.869
Light Color*Light Color	1	0.000	0.000	0.000	0.00	0.989
Interaction	3	7.540	7.540	2.513	1.77	0.174
Temp*Angle	1	0.004	0.004	0.004	0.00	0.960
Temp*Light Color	1	6.600	6.600	6.600	4.66	0.039
Angle*Light Color	1	0.936	0.936	0.936	0.66	0.423
Residual Error	29	41.075	41.075	1.416		
Lack-of-Fit	5	14.631	14.631	2.926	2.66	0.048
Pure Error	24	26.444	26.444	1.102		
Total	39	433.518				

Obs	StdOrder	Power	Fit	SE Fit	Residual	St Resid
1	32	4.451	4.133	0.375	0.318	0.28
2	11	4.241	4.133	0.375	0.108	0.10
3	31	4.657	4.133	0.375	0.525	0.46
4	27	5.138	6.140	0.710	-1.002	-1.05
5	9	3.751	4.133	0.375	-0.382	-0.34
6	29	3.621	4.133	0.375	-0.511	-0.45
7	21	11.246	11.278	0.710	-0.032	-0.03
8	5	4.960	5.856	0.710	-0.896	-0.94
9	25	5.441	5.856	0.710	-0.415	-0.43
10	2	4.226	4.207	0.710	0.019	0.02
11	30	3.468	4.133	0.375	-0.664	-0.59
12	23	11.075	10.594	0.710	0.481	0.50
13	3	10.108	10.594	0.710	-0.486	-0.51
14	1	10.669	11.278	0.710	-0.610	-0.64
15	22	6.182	4.207	0.710	1.975	2.07 R
16	8	2.121	1.698	0.710	0.423	0.44
17	28	1.927	1.698	0.710	0.229	0.24
18	6	1.414	1.354	0.710	0.061	0.06
19	12	4.757	4.133	0.375	0.625	0.55
20	26	1.308	1.354	0.710	-0.046	-0.05
21	4	4.393	3.584	0.710	0.810	0.85
22	7	5.156	6.140	0.710	-0.984	-1.03
23	24	4.094	3.584	0.710	0.511	0.53
24	10	4.078	4.133	0.375	-0.055	-0.05
25	37	7.776	5.624	0.689	2.152	2.22 R
26	20	2.805	2.632	0.413	0.173	0.16
27	35	2.330	2.873	0.689	-0.543	-0.56
28	16	3.021	2.596	0.689	0.425	0.44
29	33	13.626	11.104	0.689	2.523	2.60 R
30	39	2.663	2.632	0.413	0.031	0.03
31	38	0.532	-0.343	0.689	0.874	0.90
32	19	2.635	2.632	0.413	0.003	0.00
33	36	2.188	2.596	0.689	-0.408	-0.42
34	14	0.301	1.703	0.689	-1.402	-1.45
35	13	11.001	11.104	0.689	-0.103	-0.11
36	17	1.843	5.624	0.689	-3.781	-3.90 R
37	40	2.466	2.632	0.413	-0.166	-0.15
38	18	0.398	-0.343	0.689	0.741	0.76
39	15	3.386	2.873	0.689	0.513	0.53
40	34	0.672	1.703	0.689	-1.031	-1.06

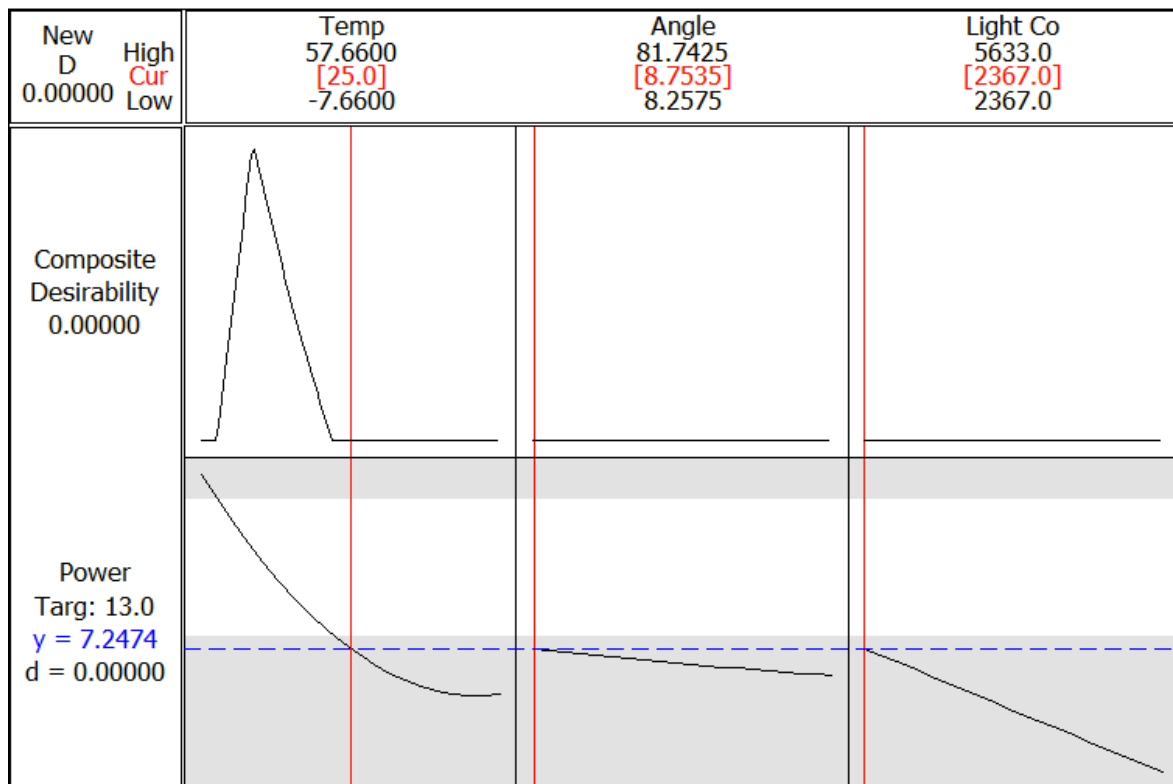
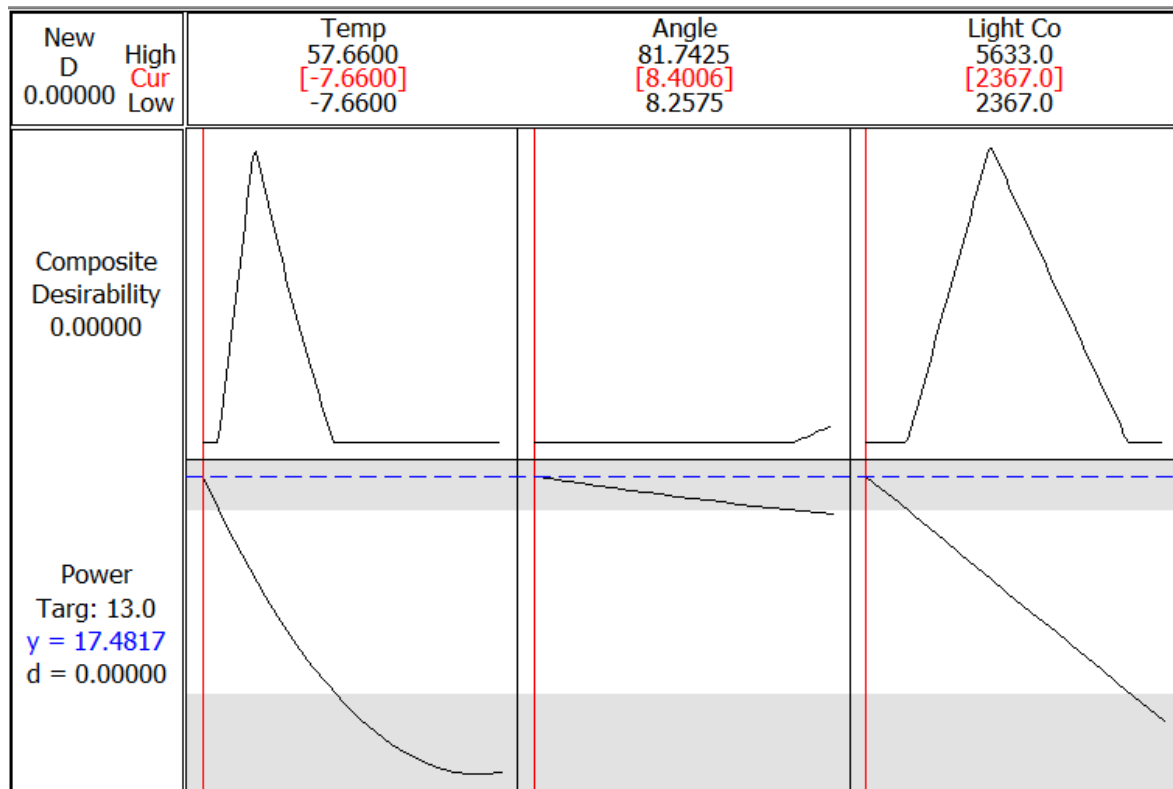
R denotes an observation with a large standardized residual.

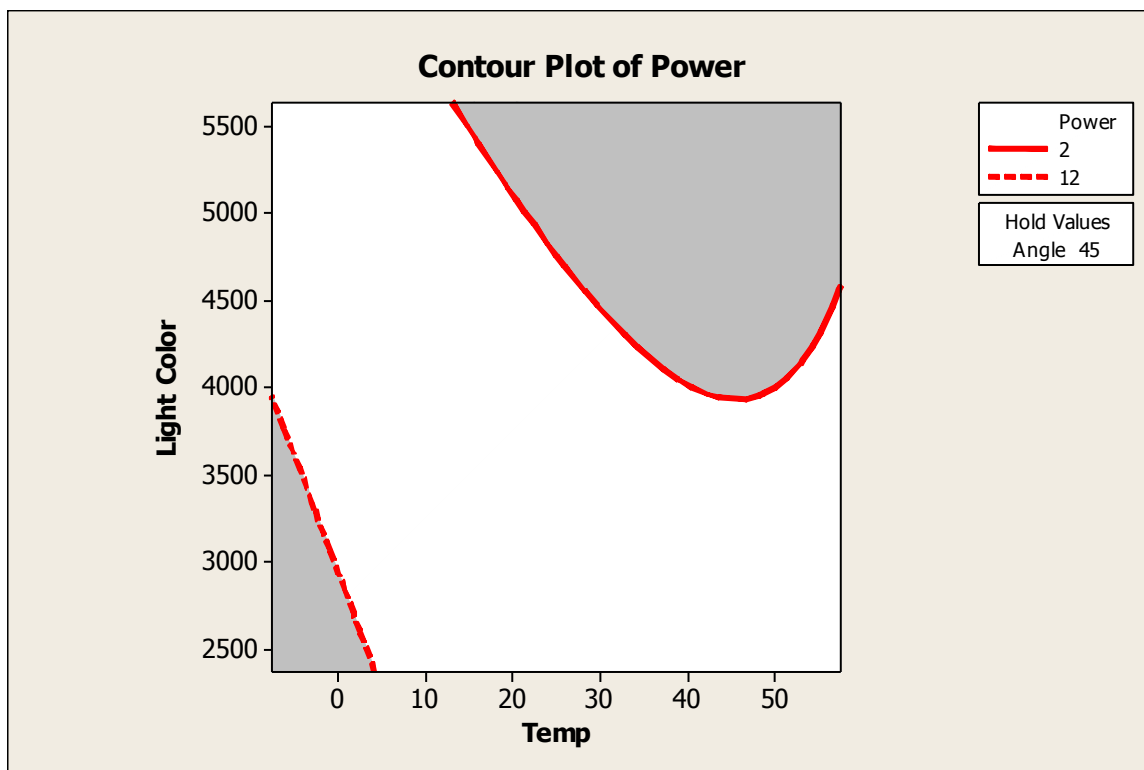
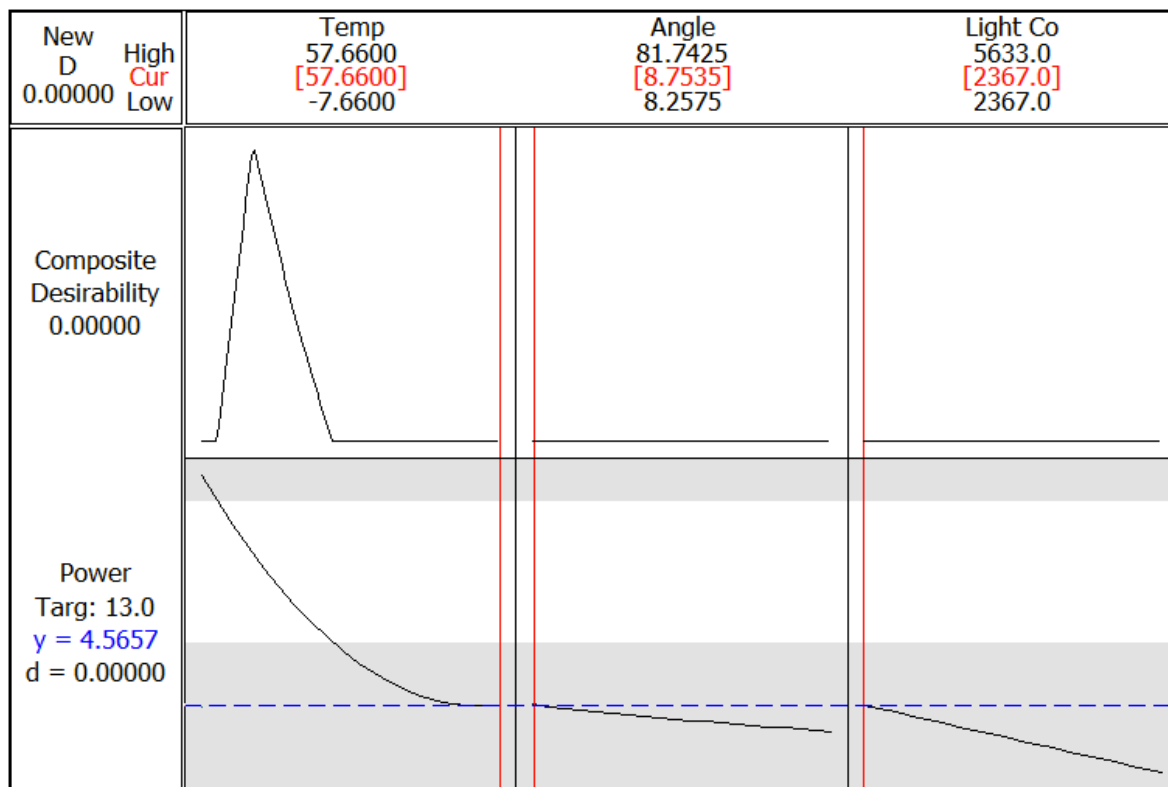
Estimated Regression Coefficients for Power using data in uncoded units

Term	Coef
Constant	22.0584
Block	0.750408
Temp	-0.450674
Angle	-0.0544616
Light Color	-0.00313979
Temp*Temp	0.00353564
Angle*Angle	7.59473E-05
Light Color*Light Color	3.27926E-09
Temp*Angle	3.38611E-05
Temp*Light Color	3.21135E-05
Angle*Light Color	1.07519E-05



Response surface optimization charts.





APPENDIX B

BBD complete results

Repeated measurements																									Avg P (W)	
StdOrder	RunOrder	Blocks	Temp	Angle	Light Color	T 1	V 1	C 1	P 1	T 2	V 2	C 2	P 2	T 3	V 3	C 3	P 3	T 4	V 4	C 4	P 4	T 5	V 5	C 5	P 5	
11	1	1	25	0	5000	25.5	10.61	0.13	1.38	25.2	10.85	0.14	1.52	26.1	10.26	0.13	1.33	26.2	10.55	0.13	1.37	27.4	10.37	0.13	1.35	1.39
29	2	1	25	45	4000	24.9	14.58	0.24	3.50	25.1	14.32	0.24	3.44	25.3	14.15	0.23	3.25	25.5	14.03	0.23	3.23	25.8	13.94	0.22	3.07	3.30
17	3	1	65	0	4000	67.7	10.38	0.06	0.62	65.2	10.33	0.06	0.62	69.5	9.83	0.05	0.49	64.3	10.15	0.05	0.51	67.7	9.82	0.05	0.49	0.55
8	4	1	65	45	5000	61.9	8.95	0.05	0.45	63.1	8.09	0.04	0.32	61.0	8.21	0.04	0.33	69.6	7.94	0.03	0.24	66.7	8.04	0.03	0.24	0.32
24	5	1	25	0	3000	24.1	19.03	0.48	9.13	24.2	18.51	0.49	9.07	24.6	18.48	0.49	9.06	25.1	18.46	0.48	8.86	26.0	18.40	0.48	8.83	8.99
15	6	1	25	45	4000	24.3	14.90	0.26	3.87	24.5	14.71	0.25	3.68	24.6	14.58	0.24	3.50	24.9	14.54	0.24	3.49	25.4	14.46	0.23	3.33	3.57
12	7	1	25	90	5000	24.6	11.97	0.20	2.39	24.9	11.85	0.19	2.25	25.1	11.80	0.19	2.24	25.7	11.62	0.18	2.09	26.2	15.59	0.18	2.81	2.36
4	8	1	65	90	4000	65.2	11.33	0.11	1.25	65.5	11.02	0.08	0.88	66.7	10.82	0.08	0.87	67.5	10.33	0.06	0.62	67.0	10.80	0.07	0.76	0.87
20	9	1	-15	45	3000	-12.3	20.85	0.60	12.51	-13.3	21.32	0.62	13.22	-13.8	21.54	0.63	13.57	-14.2	21.70	0.64	13.89	-14.5	21.79	0.64	13.95	13.43
14	10	1	25	45	4000	23.8	13.37	0.17	2.27	24.3	13.03	0.18	2.35	25.1	12.88	0.17	2.19	25.7	12.66	0.17	2.15	25.9	12.61	0.16	2.02	2.20
6	11	1	65	45	3000	65.8	16.22	0.35	5.68	69.2	14.65	0.31	4.54	67.2	14.43	0.31	4.47	65.5	14.52	0.30	4.36	64.8	14.62	0.30	4.39	4.69
25	12	1	25	90	3000	24.7	17.28	0.44	7.60	25.0	17.80	0.46	8.19	25.5	17.78	0.46	8.18	25.9	17.75	0.46	8.17	26.3	17.72	0.46	8.15	8.06
28	13	1	25	45	4000	24.8	15.18	0.28	4.25	24.9	15.10	0.28	4.23	25.1	15.04	0.28	4.21	25.2	14.98	0.26	3.89	25.5	14.94	0.26	3.88	4.09
16	14	1	-15	0	4000	-16.5	18.40	0.46	8.46	-17.5	18.82	0.47	8.85	-17.7	19.03	0.48	9.13	-18.0	19.11	0.48	9.17	-18.3	19.23	0.50	9.62	9.05
27	15	1	25	90	5000	21.5	13.10	0.24	3.14	22.2	12.88	0.24	3.09	22.8	12.69	0.23	2.92	23.5	12.47	0.22	2.74	24.0	12.39	0.22	2.73	2.92
13	16	1	25	45	4000	24.3	15.30	0.29	4.44	24.4	15.18	0.28	4.25	24.5	15.05	0.26	3.91	24.7	14.94	0.26	3.88	25.0	14.77	0.25	3.69	4.04
10	17	1	25	90	3000	24.4	18.40	0.49	9.02	25.2	18.34	0.49	8.99	26.2	18.24	0.48	8.76	26.9	18.18	0.48	8.73	27.6	18.15	0.48	8.71	8.84
18	18	1	-15	90	4000	-16.0	20.71	0.53	10.98	-17.5	21.28	0.55	11.70	-18.0	21.52	0.56	12.05	-15.4	19.28	0.49	9.45	-16.3	20.31	0.49	9.95	10.83
19	19	1	65	90	4000	68.3	10.94	0.08	0.88	64.3	10.76	0.08	0.86	67.8	10.56	0.07	0.74	62.4	10.87	0.08	0.87	63.6	10.82	0.08	0.87	0.84
2	20	1	65	0	4000	70.0	9.23	0.04	0.37	62.5	9.38	0.04	0.38	60.5	9.64	0.05	0.48	64.3	8.99	0.04	0.36	66.1	8.83	0.04	0.35	0.39
5	21	1	-15	45	3000	-12.0	21.08	0.61	12.86	-13.0	21.24	0.62	13.17	-13.9	21.41	0.63	13.49	-14.4	21.49	0.63	13.54	-14.9	21.59	0.63	13.60	13.33
30	22	1	25	45	4000	24.6	14.53	0.25	3.63	26.4	14.64	0.25	3.66	26.7	14.56	0.25	3.64	26.5	14.54	0.23	3.344	26.3	14.58	0.24	3.49	3.56
3	23	1	-15	90	4000	-15.1	21.30	0.56	11.93	-15.8	22.05	0.59	13.01	-18.4	23.29	0.61	14.21	-17.1	22.53	0.58	13.07	-15.2	22.45	0.60	13.47	13.14
22	24	1	-15	45	5000	-15.3	17.82	0.48	8.55	-15.9	18.04	0.50	9.02	-16.5	18.44	0.51	9.40	-15.8	18.00	0.48	8.64	-15.2	17.78	0.46	8.18	8.76
7	25	1	-15	45	5000	-14.3	17.40	0.45	7.83	-15.8	17.94	0.47	8.43	-17.3	18.39	0.49	9.01	-18.1	18.68	0.50	9.34	-17.7	18.53	0.49	9.08	8.74
26	26	1	25	0	5000	25.8	10.92	0.14	1.53	25.6	10.85	0.14	1.52	26.2	10.36	0.13	1.35	26.1	10.25	0.13	1.33	27.0	10.16	0.13	1.32	1.41
23	27	1	65	45	5000	70.0	9.29	0.08	0.74	65.3	9.30	0.08	0.74	62.2	9.63	0.09	0.87	63.7	9.52	0.08	0.76	65.1	9.33	0.08	0.75	0.77
9	28	1	25	0	3000	23.1	19.63	0.49	9.62	24.1	19.50	0.49	9.56	24.7	19.28	0.49	9.45	25.1	18.96	0.48	9.10	25.7	18.45	0.48	8.86	9.32
1	29	1	-15	0	4000	-17.1	20.72	0.53	10.98	-15.1	20.98	0.54	11.33	-13.7	21.08	0.54	11.38	-15.9	21.48	0.56	12.03	-17.3	21.67	0.55	11.92	11.53
21	30	1	65	45	3000	64.4	15.57	0.36	5.61	70.0	14.60	0.32	4.67	68.3	14.33	0.29	4.16	69.2	14.00	0.29	4.06	66.9	14.04	0.29	4.07	4.51
32	31	2	65	0	4000	69.7	7.33	0.05	0.38	62.6	7.45	0.05	0.39	60.9	7.64	0.07	0.50	65.1	7.14	0.05	0.37	65.9	7.28	0.05	0.38	0.40
41	32	2	25	0	5000	64.3	12.55	0.29	3.64	69.8	11.77	0.26	3.04	68.5	11.55	0.23	2.70	69.1	11.28	0.23	2.64	66.5	11.32	0.23	2.65	2.93
40	33	2	25	90	3000	24.6	13.61	0.36	4.95	25.1	14.01	0.39	5.47	26.1	14.13	0.39	5.51	26.6	14.11	0.53	7.52	27.2	14.08	0.53	7.50	6.19
36	34	2	65	45	3000	65.3	12.65	0.27	3.45	68.7	11.43	0.24	2.76	67.5	11.26	0.24	2.72	65.9	11.33	0.23	2.65	65.1	11.40	0.23	2.67	2.85
47	35	2	65	0	4000	67.4	8.10	0.07	0.53	63.1	8.06	0.07	0.52	60.9	7.67	0.05	0.40	63.7	7.92	0.05	0.41	65.8	7.66	0.05	0.40	0.45
37	36	2	-15	45	5000	-15.5	13.90	0.42	5.78	-16.2	14.07	0.49	6.95	-16.8	14.38	0.49	7.11	-15.8	14.04	0.48	6.75	-14.8	13.87	0.47	6.49	6.62
49	37	2	65	90	4000	67.7	8.53	0.06	0.53	65.3	8.39	0.06	0.52	67.2	8.24	0.05	0.45	62.8	8.48	0.06	0.53	63.8	8.44	0.06	0.53	0.51
58	38	2	25	45	4000	24.6	11.62	0.20	2.36	26.5	11.47	0.20	2.24	26.6	11.37	0.19	2.13	26.8	11.34	0.19	2.12	26.4	11.28	0.18	2.02	2.17
43	39	2	25	45	4000	24.0	11.93	0.23	2.70	24.4	11.84	0.22	2.59	25.0	11.74	0.20	2.38	25.1	11.65	0.20	2.36	25.3	11.52	0.20	2.25	2.46
56	40	2	25	0	5000	26.1	8.52	0.11	0.93	25.8	8.46	0.11	0.92	25.9	8.08	0.10	0.82	26.1	8.00	0.10	0.81	26.7	7.92	0.10	0.80	0.86
51	41	2	65	45	3000	65.3	12.14	0.28	3.41	68.7	11.39	0.25	2.84	67.5	11.18	0.23	2.53	65.6	10.92	0.23	2.47	64.6	10.95	0.23	2.48	2.75
33	42	2	-15	90	4000	-13.9	16.15	0.41	6.68	-15>-																

Box-Behnken Design

Factors: 3 Replicates: 2
Base runs: 15 Total runs: 60
Base blocks: 2 Total blocks: 2

Center points: 6

Response Surface Regression: Power versus Temp, Angle, Light Color

The analysis was done using coded units.

Estimated Regression Coefficients for Power

Term	Coef	SE Coef	T	P
Constant	3.4583	0.4005	8.636	0.000
Temp	-4.7409	0.2452	-19.332	0.000
Angle	0.3276	0.2452	1.336	0.197
Light Color	-2.7808	0.2452	-11.339	0.000
Temp*Temp	1.9238	0.3610	5.329	0.000
Angle*Angle	0.5163	0.3610	1.430	0.168
Light Color*Light Color	1.4358	0.3610	3.978	0.001
Temp*Angle	-0.3258	0.3468	-0.939	0.359
Temp*Light Color	0.1435	0.3468	0.414	0.683
Angle*Light Color	0.4864	0.3468	1.402	0.176

S = 0.980960 PRESS = 46.6031

R-Sq = 96.48% R-Sq(pred) = 91.49% R-Sq(adj) = 94.90%

Analysis of Variance for Power

Source	DF	Seq SS	Adj SS	Adj MS	F	P
Regression	9	528.186	528.186	58.687	60.99	0.000
Linear	3	485.059	485.059	161.686	168.02	0.000
Temp	1	359.619	359.619	359.619	373.71	0.000
Angle	1	1.717	1.717	1.717	1.78	0.197
Light Color	1	123.722	123.722	123.722	128.57	0.000
Square	3	40.220	40.220	13.407	13.93	0.000
Temp*Temp	1	23.772	27.329	27.329	28.40	0.000
Angle*Angle	1	1.224	1.969	1.969	2.05	0.168
Light Color*Light Color	1	15.224	15.224	15.224	15.82	0.001
Interaction	3	2.907	2.907	0.969	1.01	0.410
Temp*Angle	1	0.849	0.849	0.849	0.88	0.359
Temp*Light Color	1	0.165	0.165	0.165	0.17	0.683
Angle*Light Color	1	1.893	1.893	1.893	1.97	0.176
Residual Error	20	19.246	19.246	0.962		
Lack-of-Fit	3	10.460	10.460	3.487	6.75	0.003
Pure Error	17	8.786	8.786	0.517		
Total	29	547.431				

Obs	StdOrder	Power	Fit	SE Fit	Residual	St Resid
1	11	1.390	1.816	0.601	-0.425	-0.55
2	29	3.297	3.458	0.400	-0.161	-0.18
3	17	0.547	1.156	0.601	-0.609	-0.79
4	8	0.316	-0.560	0.601	0.876	1.13
5	24	8.990	8.350	0.601	0.640	0.83
6	15	3.573	3.458	0.400	0.115	0.13
7	12	2.357	3.444	0.601	-1.087	-1.40
8	4	0.874	1.159	0.601	-0.285	-0.37
9	20	13.426	14.483	0.601	-1.057	-1.36
10	14	2.196	3.458	0.400	-1.263	-1.41
11	6	4.687	4.714	0.601	-0.027	-0.04
12	25	8.057	8.032	0.601	0.025	0.03
13	28	4.094	3.458	0.400	0.635	0.71
14	16	9.046	9.986	0.601	-0.940	-1.21
15	27	2.925	3.444	0.601	-0.519	-0.67
16	13	4.035	3.458	0.400	0.577	0.64
17	10	8.839	8.032	0.601	0.807	1.04
18	18	10.826	11.293	0.601	-0.467	-0.60
19	19	0.842	1.159	0.601	-0.317	-0.41
20	2	0.388	1.156	0.601	-0.768	-0.99
21	5	13.331	14.483	0.601	-1.152	-1.49
22	30	3.555	3.458	0.400	0.097	0.11
23	3	13.136	11.293	0.601	1.844	2.38 R
24	22	8.759	8.635	0.601	0.125	0.16
25	7	8.739	8.635	0.601	0.104	0.13
26	26	1.410	1.816	0.601	-0.406	-0.52
27	23	0.772	-0.560	0.601	1.333	1.72
28	9	9.316	8.350	0.601	0.965	1.24
29	1	11.528	9.986	0.601	1.542	1.99
30	21	4.513	4.714	0.601	-0.201	-0.26
31	2	0.403	0.683	0.399	-0.280	-0.54
32	11	2.932	2.049	0.399	0.883	1.71
33	10	6.191	5.630	0.399	0.561	1.09
34	6	2.851	2.997	0.399	-0.146	-0.28
35	17	0.452	0.683	0.399	-0.231	-0.45
36	7	6.616	5.768	0.399	0.849	1.65
37	19	0.512	0.478	0.399	0.034	0.07
38	28	2.174	2.104	0.266	0.070	0.12
39	13	2.455	2.104	0.266	0.351	0.59
40	26	0.858	2.049	0.399	-1.192	-2.31 R
41	21	2.746	2.997	0.399	-0.251	-0.49
42	3	6.587	7.034	0.399	-0.447	-0.87
43	12	1.434	2.061	0.399	-0.627	-1.22
44	22	5.317	5.768	0.399	-0.451	-0.88
45	1	5.504	6.303	0.399	-0.799	-1.55
46	20	9.036	9.327	0.399	-0.291	-0.56
47	24	5.668	5.115	0.399	0.553	1.07
48	5	8.798	9.327	0.399	-0.529	-1.03
49	23	0.470	-0.079	0.399	0.549	1.06
50	9	5.470	5.115	0.399	0.355	0.69
51	16	7.014	6.303	0.399	0.711	1.38
52	14	2.006	2.104	0.266	-0.098	-0.17
53	4	0.532	0.478	0.399	0.054	0.10
54	27	1.779	2.061	0.399	-0.281	-0.55
55	15	1.336	2.104	0.266	-0.768	-1.29
56	30	2.163	2.104	0.266	0.059	0.10
57	29	2.491	2.104	0.266	0.387	0.65
58	25	5.378	5.630	0.399	-0.252	-0.49
59	8	0.192	-0.079	0.399	0.271	0.53
60	18	7.992	7.034	0.399	0.958	1.86

R denotes an observation with a large standardized residual.

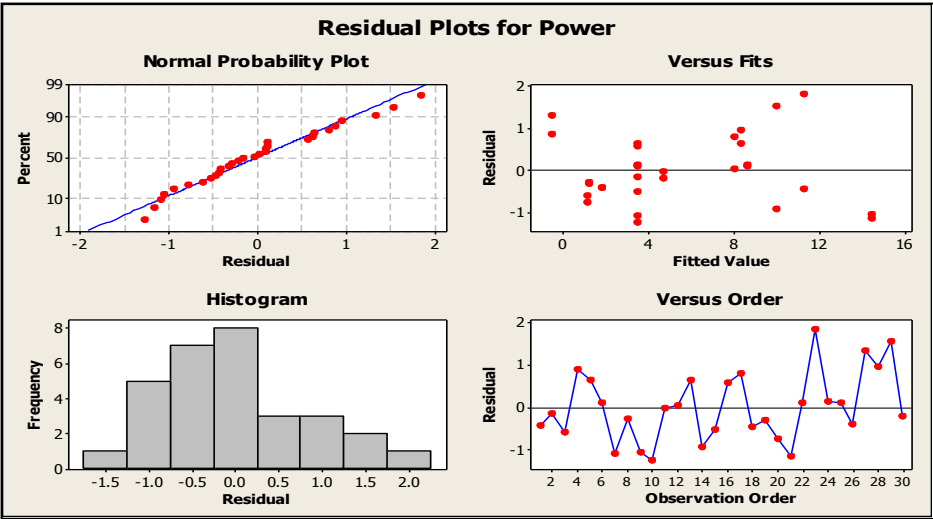
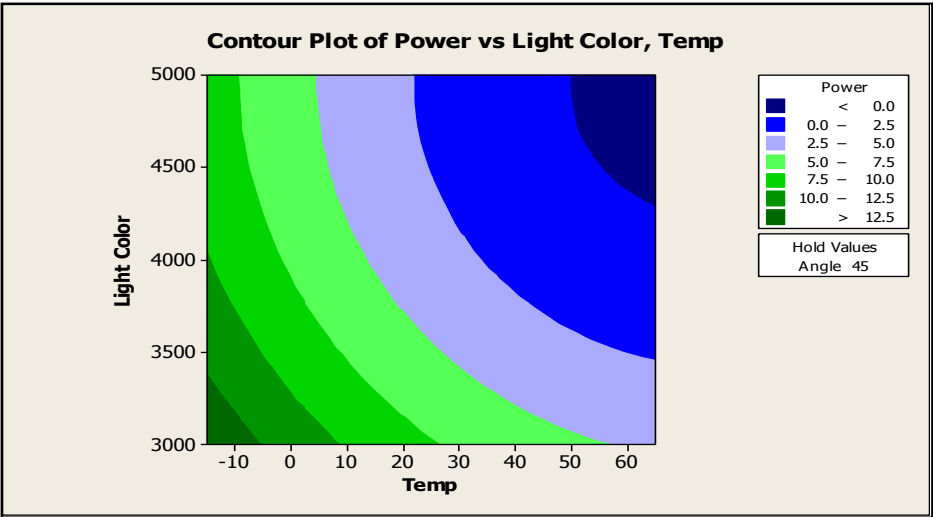
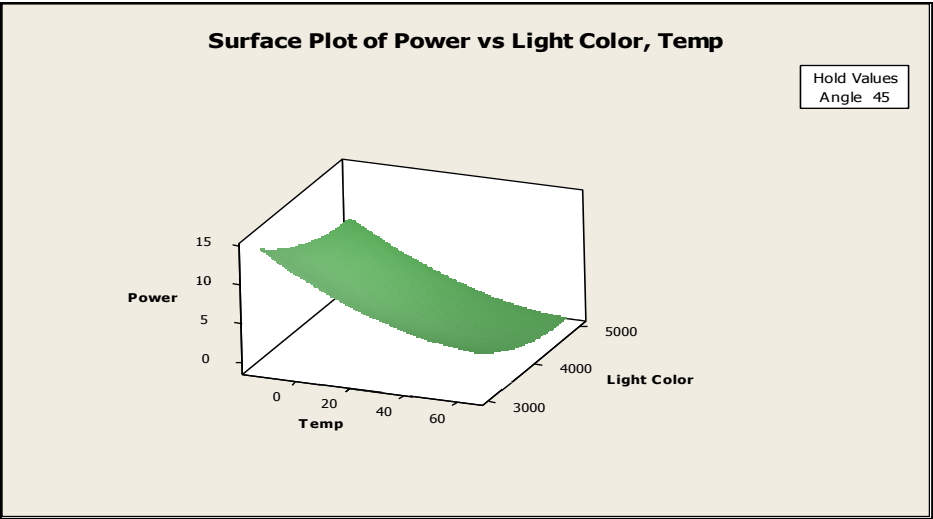
Estimated Regression Coefficients for Power using data in uncoded units

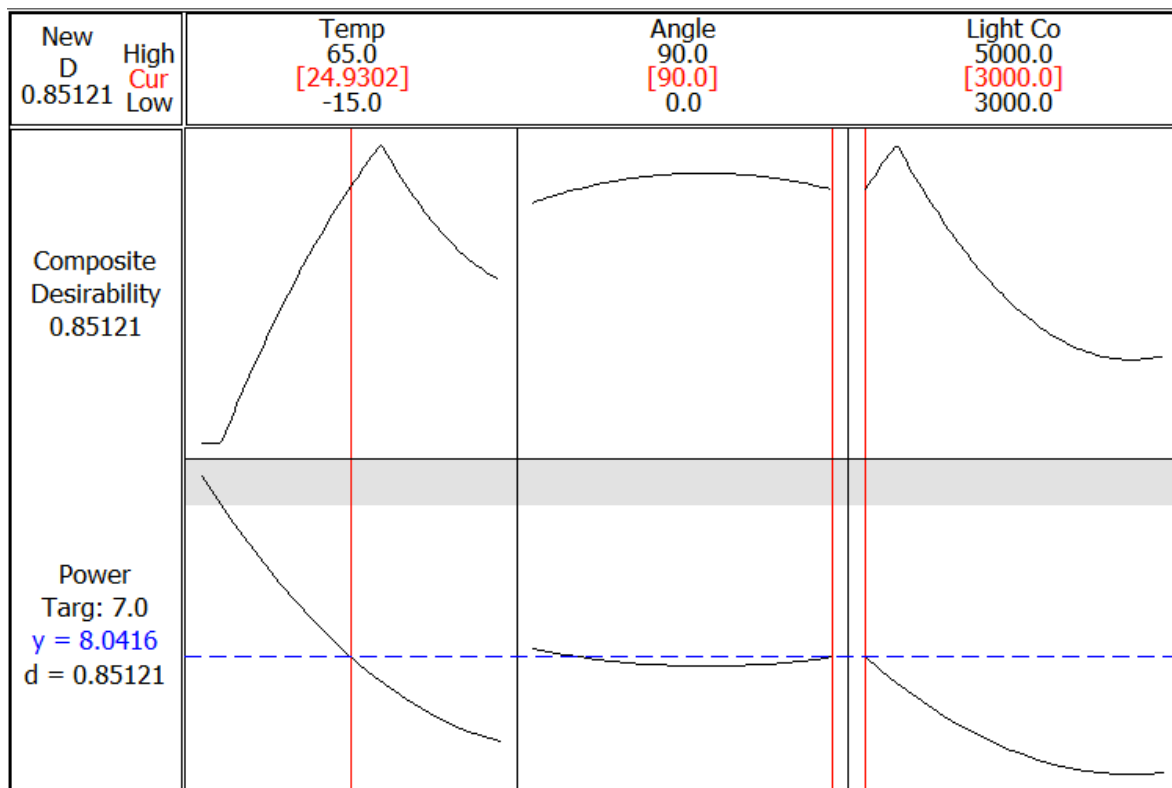
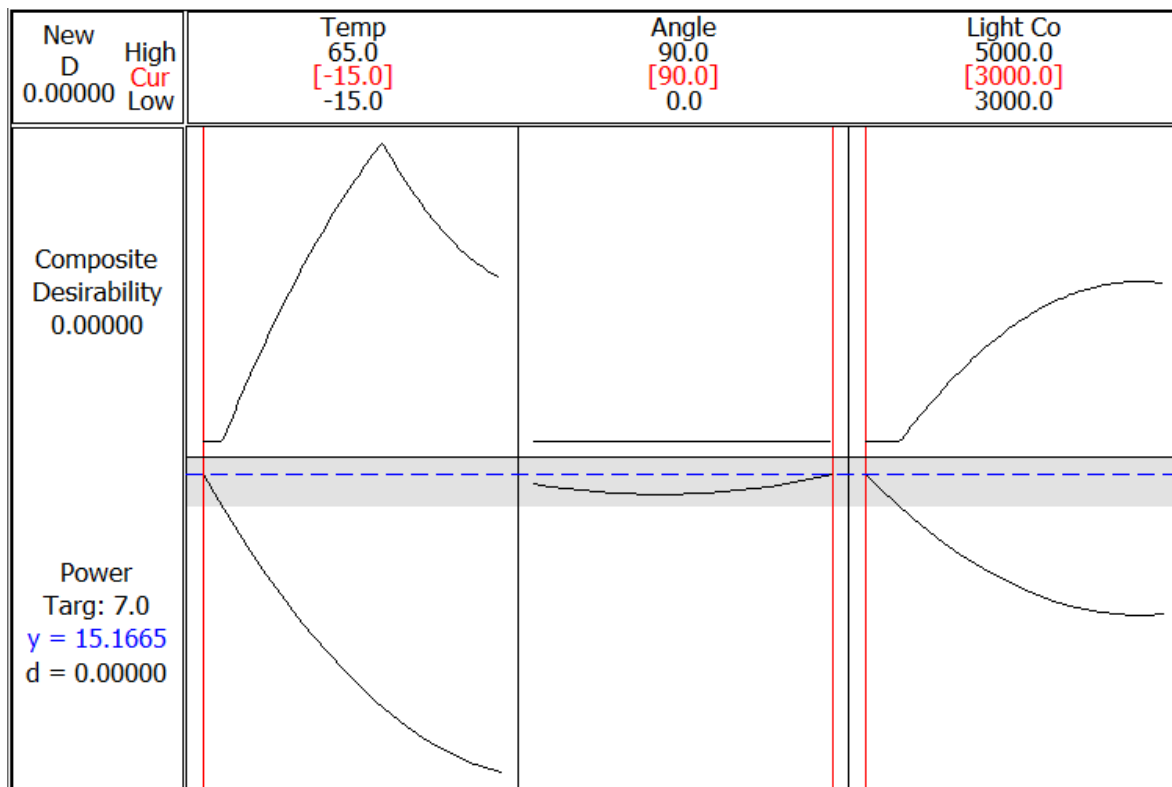
Term	Coef
Constant	43.5590
Temp	-0.184849
Angle	-0.0543797
Light Color	-0.0148436
Temp*Temp	0.00120234
Angle*Angle	0.000254981
Light Color*Light Color	1.43584E-06
Temp*Angle	-1.80994E-04
Temp*Light Color	3.58850E-06
Angle*Light Color	1.08091E-05

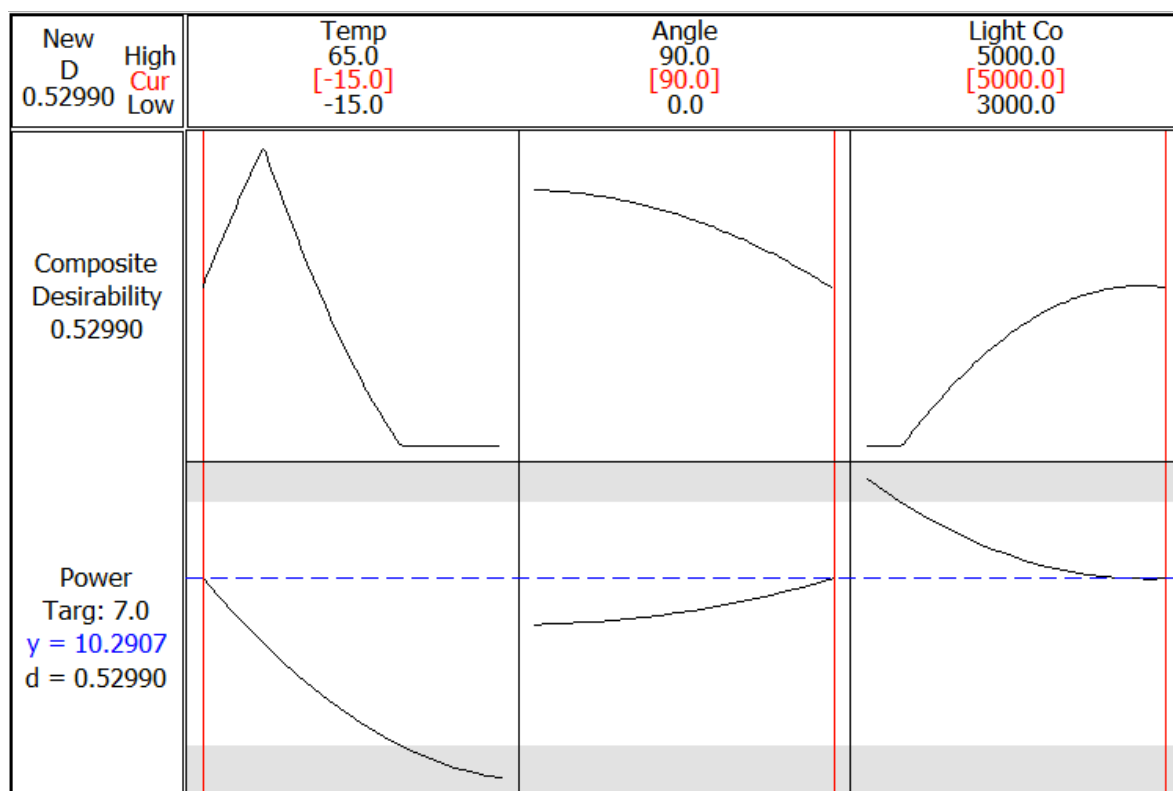
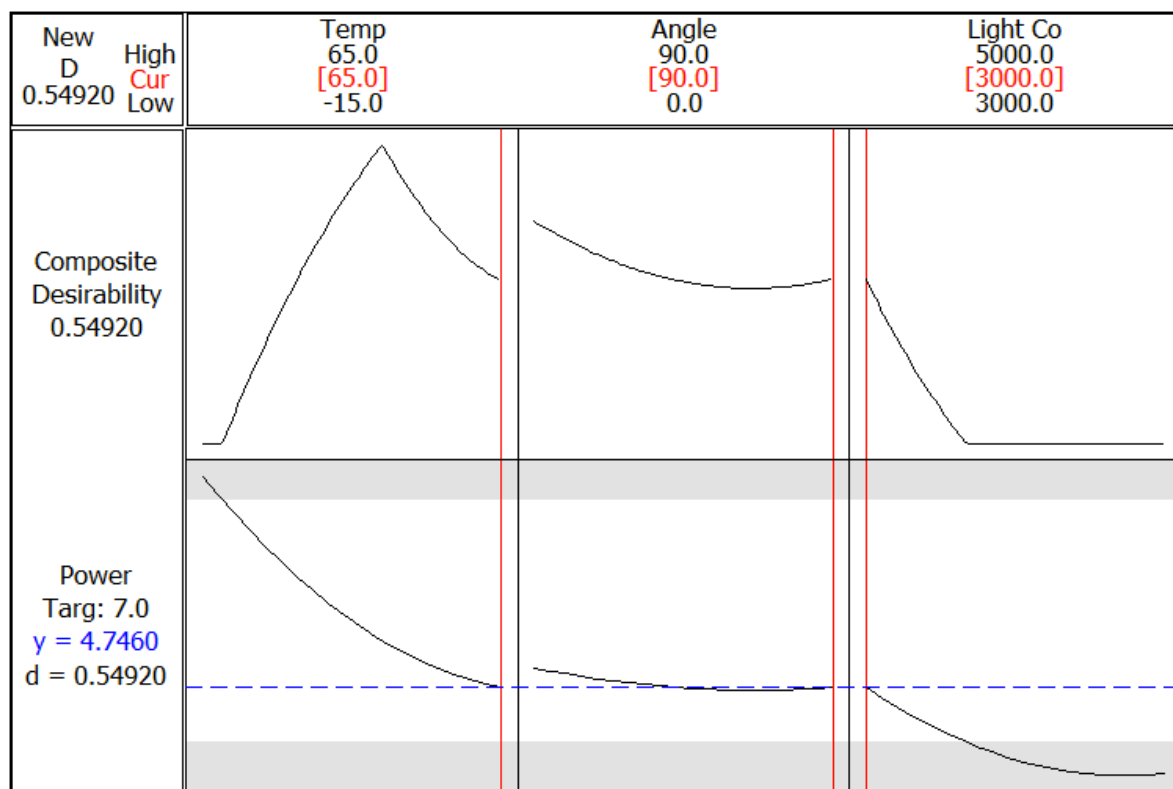
Design Table (randomized)

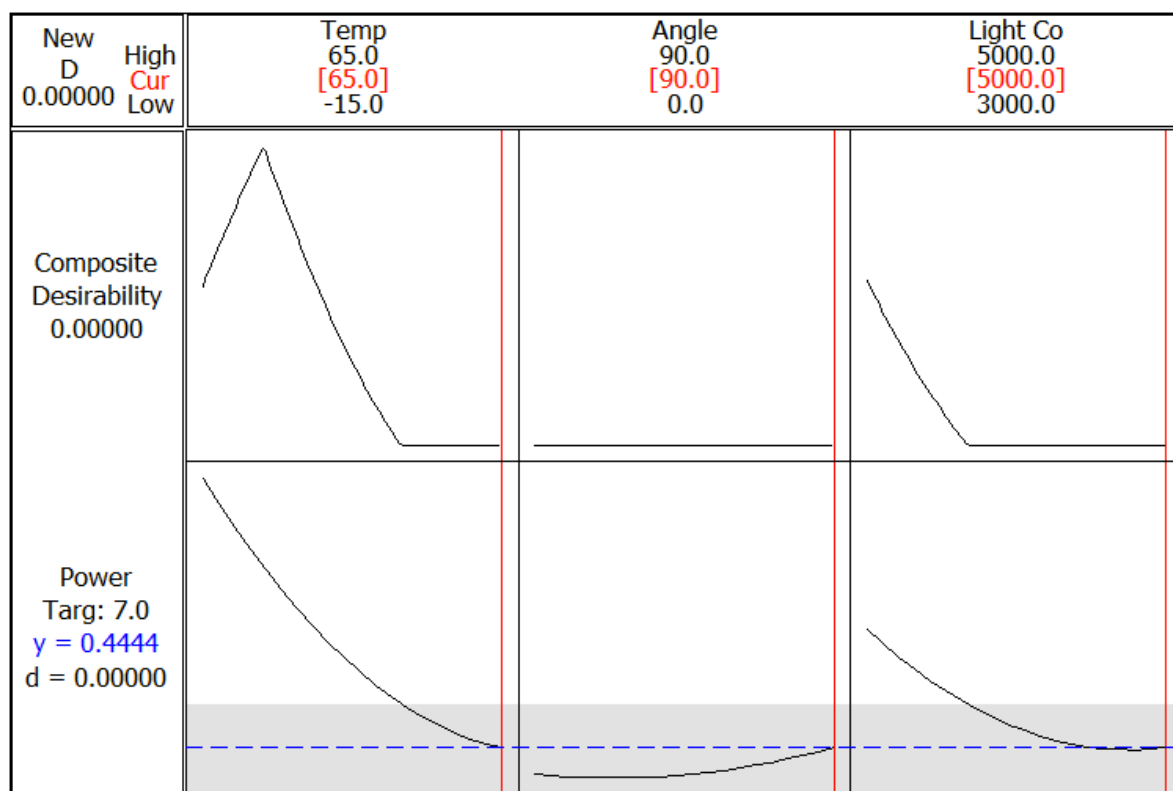
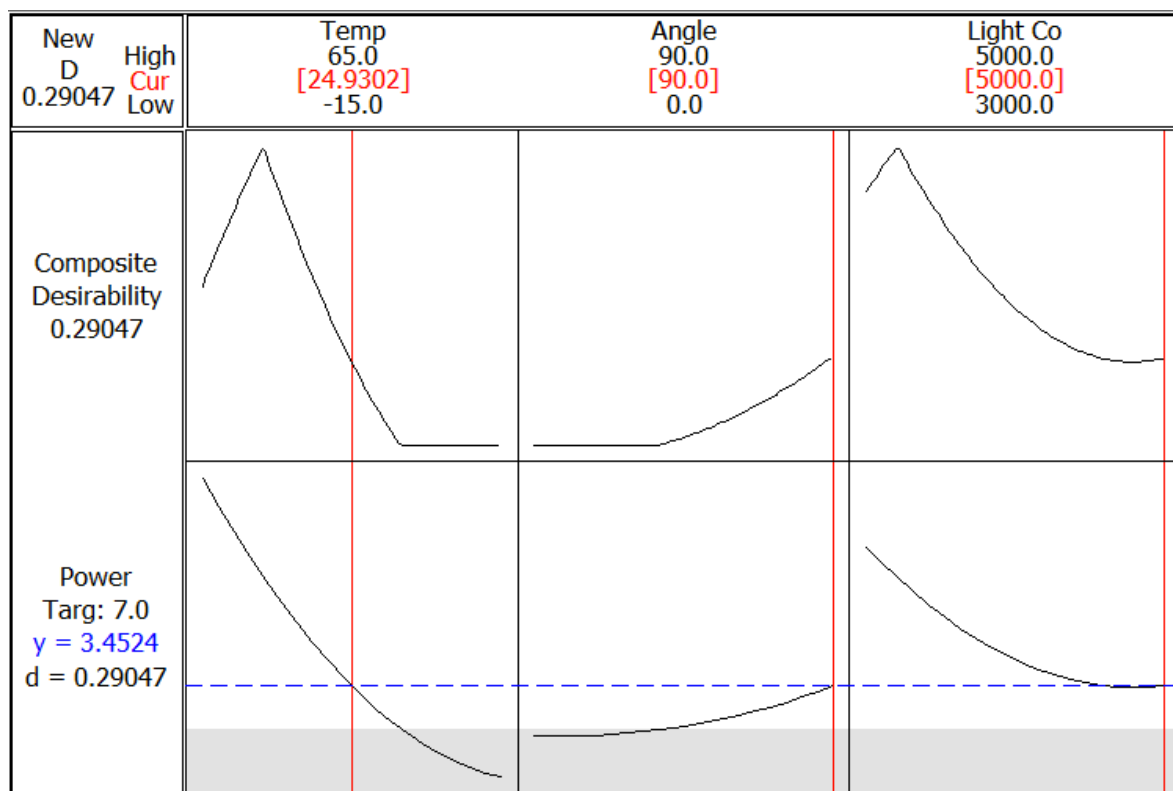
Run	Blk	A	B	C
1	1	0	-	+
2	1	0	0	0
3	1	+	-	0
4	1	+	0	+
5	1	0	-	-
6	1	0	0	0
7	1	0	+	+
8	1	+	+	0
9	1	-	0	-
10	1	0	0	0
11	1	+	0	-
12	1	0	+	-
13	1	0	0	0
14	1	-	-	0
15	1	0	+	+
16	1	0	0	0
17	1	0	+	-
18	1	-	+	0
19	1	+	+	0
20	1	+	-	0
21	1	-	0	-
22	1	0	0	0
23	1	-	+	0
24	1	-	0	+
25	1	-	0	+
26	1	0	-	+
27	1	+	0	+
28	1	0	-	-
29	1	-	-	0
30	1	+	0	-

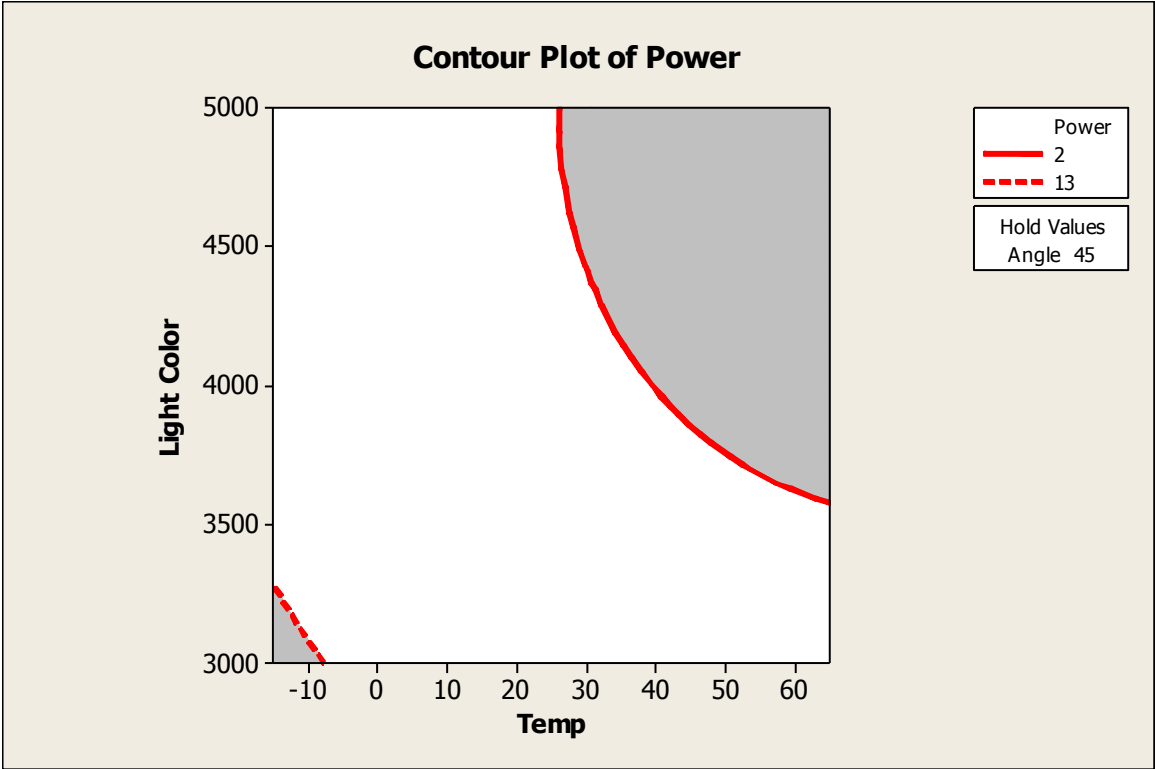
Run	Blk	A	B	C
31	2	+	-	0
32	2	0	-	+
33	2	0	+	-
34	2	+	0	-
35	2	+	-	0
36	2	-	0	+
37	2	+	+	0
38	2	0	0	0
39	2	0	0	0
40	2	0	-	+
41	2	+	0	-
42	2	-	+	0
43	2	0	+	+
44	2	-	0	+
45	2	-	-	0
46	2	-	0	-
47	2	0	-	-
48	2	-	0	-
49	2	+	0	+
50	2	0	-	-
51	2	-	-	0
52	2	0	0	0
53	2	+	+	0
54	2	0	+	+
55	2	0	0	0
56	2	0	0	0
57	2	0	0	0
58	2	0	+	-
59	2	+	0	+
60	2	-	+	0







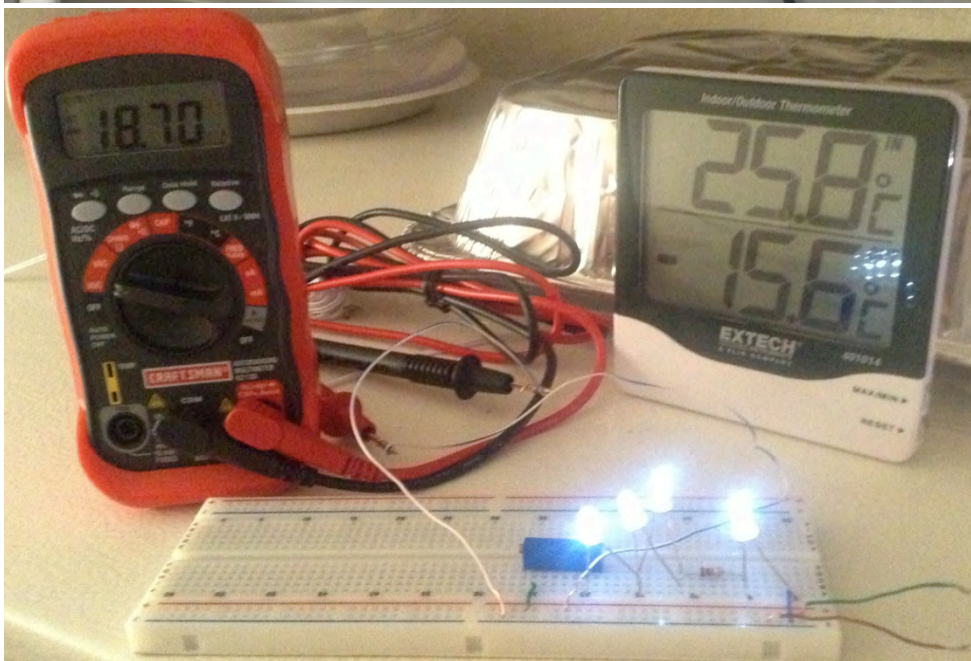




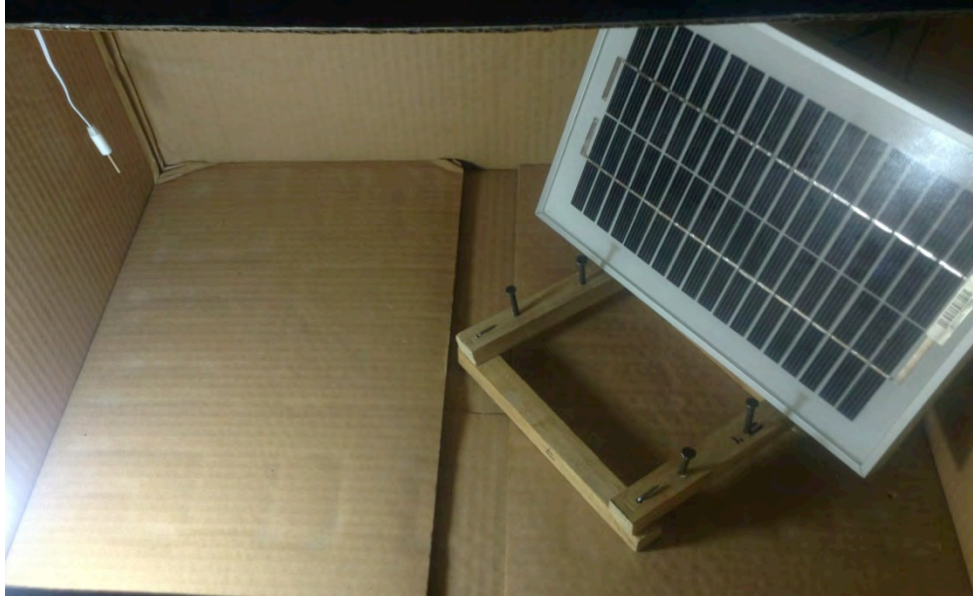
APPENDIX C

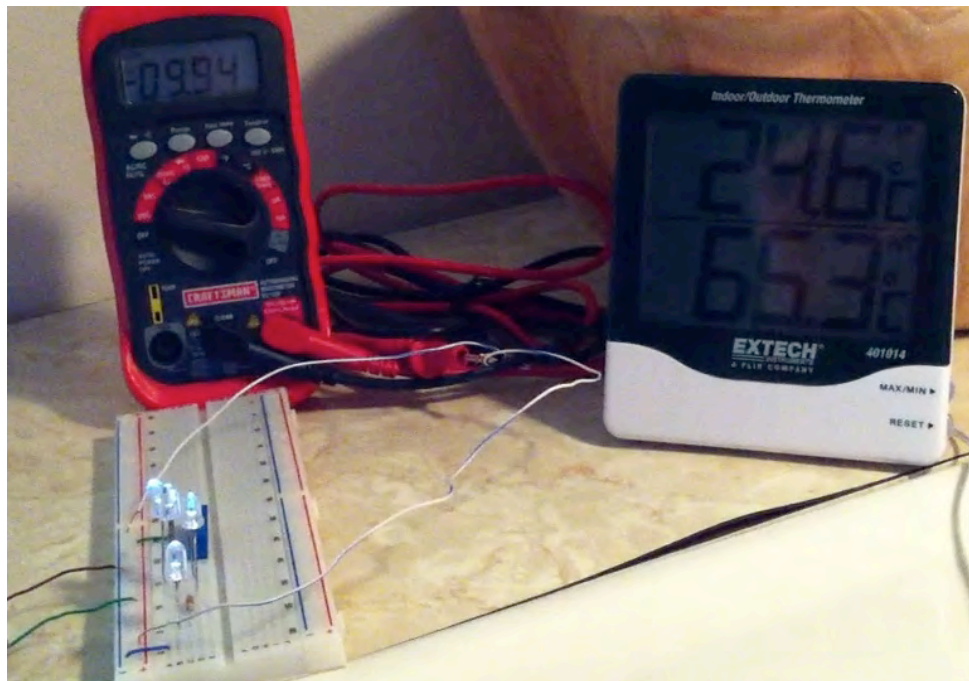
Pictures of the experiment











CURRICULUM VITA

Juan Venegas Méndez was born in Guadalajara, Jalisco, México. The first son of Juan Venegas Gonzalez and Monica Mendez Curiel, he graduated from Colegio Cervantes Bachillerato, Zapopan, Jalisco, Mexico, in the spring of 2002 and entered to the Instituto Tecnológico y de Estudios Superiores de Occidente (ITESO) to fulfill his bachelor's degree in Industrial Engineering. While pursuing the bachelor's degree, he worked at COPO, an injection molding company, as a part time production engineer for 4 years, after receiving his bachelors of Science degree from ITESO in 2007.

He was also a Jr. Consultant for 2 years for FOJAL and ITESO after his graduation until 2009 when he starts working as a production supervisor on Alen de Occidente.

After that, he worked as a Quality Manager for KIOTO Clear Energy also in Guadalajara Jalisco until he entered The University Of Texas At El Paso in 2011 when he starts his Master's degree.

He received his Master in Science in Manufacturing Engineering degree on August 2013 from The University Of Texas At El Paso.

Permanent Address:

Av. Las Fuentes 101-B
Zapopan, Jalisco. 45070